LOAD-TRANSFER AND LOAD-DIFFUSION IN ELASTOSTATICS

ELI STERNBERG
California Institute of Technology

Reprinted from
Proceedings of the
SIXTH U.S. NATIONAL CONGRESS OF APPLIED MECHANICS
Published by
The American Society of Mechanical Engineers
United Engineering Center
345 East 47th Street, New York, N.Y. 10017
Printed in U.S.A.

LOAD-TRANSFER AND LOAD-DIFFUSION IN ELASTOSTATICS*

ELI STERNBERG
California Institute of Technology

ABSTRACT

This paper summarizes a recent sequence of theoretical investigations of plane and spatial load-transfer problems in linear elastostatics. Whereas the two-dimensional problems dealt with here have a particular relevance to aircraft structures, those concerning the transfer of load between a bar and a three-dimensional elastic medium are primarily of interest in connection with civil engineering structures and have a bearing on the mechanics of fiber-reinforced materials. An attempt is made to assess the role of alternative mathematical models in the treatment of the physical problems under consideration, to sketch the essential features of the required analysis, and to discuss the principal results obtained.

INTRODUCTION

In a very broad and equally obvious sense, *all* problems involving mechanically induced stresses and deformations in elastic solids are load-transfer problems of one kind or another. The term "load-transfer" is used here in a much narrower connotation: it alludes to the mechanical interaction between two homogeneous and isotropic elastic bodies of possibly distinct material properties, which are bonded throughout a common portion of their boundaries and are in equilibrium under externally applied loads. Further, the present considerations are confined to linearly elastic materials in the presence of infinitesimal deformations. Finally, with the exception of the problem of bonded overlapping sheets, we limit ourselves to circumstances in which one of the two contiguous bodies is a "bar" that, for the purpose at hand, may be regarded as an essentially one-dimensional elastic continuum.

Plane load-transfer problems, such as those encountered in connection with plate-stringer assemblies or lap-joined sheets, are of primary importance to the stress analysis of aircraft structures. The history of problems in this category is long, elaborate, and at times bewildering: it appears to have its origins in a classical paper by Melan [1] (1932) on the diffusion of an axial load from an infinite stringer into a coplanar elastic sheet. In contrast, the more complicated *spatial* problems concerning the transfer of load from, or the load-absorption by, an elastic rod which is immersed in a three-dimensional elastic matrix, have until recently received relatively little analytical attention. The interest in load-transfer problems within this second class stems partly from civil engineering because of their relevance to the mechanics of anchor bars and pile-supported foundations. In addition, such problems have a direct bearing on the mechanics of fiber-reinforced composites, which have during the last decade gained technological prominence and have become the object of numerous experimental and theoretical investigations.

It should be made plain from the outset that this paper is not intended as a general survey of the literature on load-transfer problems of the type described above. Our objective is both less ambitious and more

*This paper was prepared under Contract Nonr-220(58) with the Office of Naval Research in Washington, D.C.

self-centered: we aim merely at a unified summary – unencumbered by tiresome detail – of the methods used and the most pertinent results obtained in a recent sequence of analytical studies conducted by the author in collaboration with Rokuro Muki.

In Section 1, which is predominantly based on [2], we first recall – in a manner suited to our purposes – Melan's [1] formulation of his two basic plane load-transfer problems. Subsequently, we discuss more refined treatments of one of Melan's problems, which pertains to the transmission of an axial load from an edge-stiffener to a semi-infinite elastic sheet. Section 2 deals with the load-exchange between two bonded overlapping sheets and is a résumé of some of the results deduced in [3]. In Section 3 we turn to the plane problem occasioned by the load-transfer from a transverse tension bar to a semi-infinite sheet. The material included in this section is chiefly drawn from [4].

The remainder of the paper is devoted to the load-transfer between a bar and a three-dimensional elastic medium. Section 4 contains in, hopefully, improved form the main features of a pilot study [5] of such problems. This section concerns the diffusion of an axial load from an infinite bar that is fully embedded in an all-around infinite elastic matrix. In Section 5, which rests on [6], the approximative scheme established in [5] and described in Section 4 is applied to the load-diffusion into a half-space from a partially embedded axially loaded rod. Finally, Section 6 is a condensed version of [7], where the method developed in [5] is used to cope with the load-absorption by a single semi-infinite filament that reinforces an elastic matrix occupying the remainder of the space.

1. MELAN'S PROBLEMS AND SOME REFINEMENTS OF MELAN'S ANALYSIS

The two fundamental plane load-transfer problems considered by Melan [1] both relate to the diffusion of an axial load from an infinite stringer of arbitrary uniform cross section into a coplanar sheet of constant thickness, the applied load being confined to, and uniformly distributed over, one of the cross sections of the stringer. In what we choose to call here Melan's first problem[1] (Fig. 1a), the sheet extends to infinity in all directions; in the second problem (Fig. 1b), the stringer is fastened to the edge of a semi-infinite sheet. Melan's analysis rests on the following basic approximative assumptions:

[1] This problem is actually taken up last in [1] and is referred to in [2] as "Melan's second problem."

(i) the stringer is regarded as a one-dimensional elastic continuum, the bending stiffness of which is neglected in the second problem

(ii) the sheet is treated as a two-dimensional elastic continuum according to the conventional theory of generalized plane stress

(iii) the bond between sheet and stringer is taken to be perfect and continuous

(iv) in the first problem the stringer attachment is modeled as an ideal line-contact

We proceed now to a mathematical formulation of Melan's problems on the basis of the foregoing hypotheses. This formulation, though different from, is equivalent to the one underlying [1] and is more instructive for our purposes. Let E, ν and E_s, ν_s denote Young's modulus and Poisson's ratio of the sheet and the stringer, respectively. Further, let h and A designate the sheet-thickness and the cross-sectional area of the stringer. Next, choose

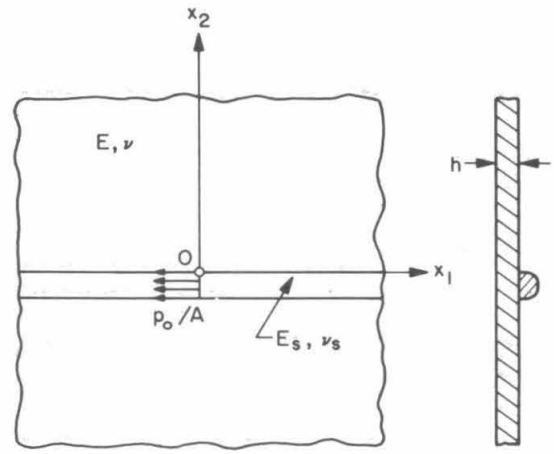

(a) FIRST PROBLEM

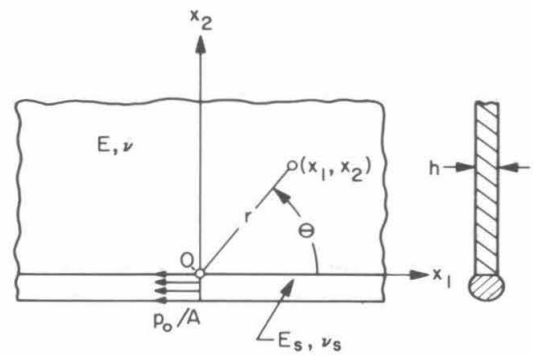

(b) SECOND PROBLEM

FIG. 1 MELAN'S PROBLEMS

rectangular cartesian coordinates (x_1, x_2) as indicated in Fig. 1 and suppose p_o is the magnitude of the resultant stringer-load, which is applied within the cross section situated at $x_1 = 0$, in the negative x_1-direction. We initially replace the given load by a statically equivalent distributed axial loading that vanishes outside a stringer segment of length 2δ centered at the origin, with a view toward ultimately passing to the limit as $\delta \to 0$. If $f(x)$ stands for the lineal density of this "replacement loading" at $x_1 = x$, we thus require

$$f(x) < 0 \ (-\delta < x < \delta), \ f(x) = 0 \ (\delta \leq |x| < \infty) \tag{1.1}$$

$$f(-x) = f(x) \ (-\infty < x < \infty), \ \int_{-\delta}^{\delta} f(x)dx = -p_o .$$

In addition we demand that f be suitably smooth[2] on the entire real axis. By virtue of assumption (i), the stringer obeys the *stress-strain relation*

$$\frac{p(x)}{A} = \sigma(x) = E_s \, \epsilon(x) \ (-\infty < x < \infty) \tag{1.2}$$

and is governed by the one-dimensional *differential equation of equilibrium*

$$p'(x) + q(x) + f(x) = 0 \ (-\infty < x < \infty), \tag{1.3}$$

provided $p(x)$ is the scalar axial force in the stringer at $x_1 = x$, $\sigma(x)$ and $\epsilon(x)$ are the corresponding normal stress and extensional strain, while $q(x)$ is the scalar bond-force per unit length exerted by the sheet upon the stringer at the same location.

At this stage we limit our attention temporarily to Melan's first problem (Fig. 1a). Because of assumptions (ii), (iv), the bond-forces acting upon the sheet constitute a line-load of scalar lineal density $-q$ applied along the x_1-axis. Hence (ii), (iii), (iv) furnish the *kinematic bond condition*

$$\epsilon(x) = \int_{-\infty}^{\infty} q(\xi) \, \mathring{\epsilon}(x - \xi) \, d\xi \ (-\infty < x < \infty), \tag{1.4}$$

where $\mathring{\epsilon}(x)$ is the thickness-average, based on the theory of generalized plane stress, of the extensional sheet strain parallel to the x_1-axis at the point $(x, 0)$, due to a unit concentrated load applied at the origin in the negative x_1-direction. This influence function is well known and is given by[4]

$$\mathring{\epsilon}(x) = \frac{(3-\nu)(1+\nu)}{4\pi hEx} \ (0 < |x| < \infty). \tag{1.5}$$

On setting

$$\lambda = \frac{4hE}{A(3-\nu)(1+\nu)E_s}, \tag{1.6}$$

equations (1.2) to (1.6) yield at once

$$\lambda p(x) + \frac{1}{\pi} \int_{-\infty}^{\infty} \frac{p'(\xi) + f(\xi)}{x - \xi} \, d\xi = 0 \ (-\infty < x < \infty), \tag{1.7}$$

in which the integral is to be interpreted in the sense of its Cauchy principal value. The singular integro-differential equation (1.7) for the desired stringer-force p has a translation kernel and is readily solved with the aid of the exponential Fourier transform. Passing to the limit as $\delta \to 0$ in the solution thus obtained, and bearing (1.1) in mind, one finds that

$$p(x) = \frac{p_o}{2} \left\{ \cos(\lambda x) \left[1 - \frac{2}{\pi} Si(\lambda x) \right] + \frac{2}{\pi} \sin(\lambda x) Ci(\lambda x) \right\} \ (0 < x < \infty), \tag{1.8}$$

where Si and Ci are the familiar sine and cosine integrals. From (1.8) one easily draws the estimates

$$p(x) = \frac{p_o}{2} + o(1) \text{ as } x \to 0, \ p(x) = \frac{p_o}{\pi \lambda x} + o(x^{-1}) \text{ as } x \to \infty,$$

$$p'(x) = \frac{p_o \lambda}{\pi} \log(x/\sqrt{A}) + O(1) \text{ as } x \to 0. \tag{1.9}$$

Turning to Melan's second problem (Fig. 1b), we recall again assumption (i) and note that the neglect of the stringer's bending stiffness implies the vanishing of the normal tractions on the interface between the semi-infinite sheet and the stringer (edge-stiffener). Consequently, (1.4) remains valid for the second problem, provided $\mathring{\epsilon}(x)$ is at present the thickness-average of the extensional sheet strain parallel to the x_1-axis at the point $(x, 0)$, due to a unit concentrated tangential load applied at the origin in the negative x_1-direction. The new influence function $\mathring{\epsilon}$

[1] Strictly speaking (1.1) introduces a one-parameter *family* of replacement loadings, depending on the parameter δ.

[2] In keeping with the character of this paper we shall refrain from stating the explicit regularity hypotheses needed to justify the analysis at hand.

[3] Throughout this paper a prime attached to a symbol denoting a function of one variable indicates differentiation.

[4] See, for example, Girkmann[8], art. 47.

[5] Because of symmetry it is sufficient to consider only $p(x)$ for $x > 0$.

is available from the appropriate generalized plane-stress solution[1] for the half-plane and has the form

$$\overset{\circ}{\epsilon}(x) = \frac{2}{\pi h E x} \quad (0 < |x| < \infty). \tag{1.10}$$

It follows that (1.7), and hence (1.8), continues to hold in the present circumstances if the definition of the parameter λ in (1.6) is replaced by

$$\lambda = \frac{hE}{2AE_s}. \tag{1.11}$$

Once the stringer-force p is known, so is the loading communicated to the sheet, and therefore the explicit determination of the sheet stresses in either of Melan's problems is now an elementary task which need not be pursued further at this point.[2]

In the special case of a stringer of rectangular cross section – say, of thickness h_s and width a (see the inset diagram in Fig. 2) – Melan's second problem is amenable to a rigorous two-dimensional treatment, in which the theory of generalized plane stress is applied strictly to the sheet and the edge-stiffener alike. This "exact" solution, deduced in [2],[3] is physically relevant only if h_s/a and h/a are both sufficiently small compared to unity. Further, regardless of the shape of the stringer cross section, Melan's approximate analysis of the second problem may be refined by taking into account the flexural rigidity of the stiffener within the framework of the elementary beam theory. For a rectangular stiffener cross section such an improved approximate solution, also established in [2], is intermediate between Melan's and the exact solution referred to above.

We now summarize briefly the most significant conclusions reached in [2] on the basis of the foregoing three alternative treatments of Melan's second problem.[4] The stringer-force p in *all three solutions* is found to obey the asymptotic estimates

$$\begin{aligned} p(x) &= \frac{p_o}{2} + o(1) \text{ as } x \to 0, \\ p(x) &= \frac{2p_o \kappa a}{\pi x}\,[1 + O(x^{-2})] \text{ as } x \to \infty, \end{aligned} \tag{1.12}$$

where κ is the stiffness-ratio given by

$$\kappa = \frac{h_s E_s}{hE}. \tag{1.13}$$

Also, all three solutions predict that $p'(x)$ becomes logarithmically unbounded as $x \to 0$. This fact is reflected in the infinite initial slope of the load-diffusion curves presented in Fig. 2. As is apparent from this figure, the values of p predicted by the alternative solutions under comparison are in good agreement over the entire range of the stringer, and the agreement becomes progressively more favorable as the stiffness-ratio is increased.

Similarly, the choice of the stringer model has little influence upon the *far-field* behavior of the sheet stresses $\sigma_{\alpha\beta}(\alpha, \beta = 1, 2)$. If (r, θ) are the polar coordinates indicated in Fig. 1b, one has in *all three instances*

$$\begin{aligned} \sigma_{11} &= \frac{2p_o}{\pi h}\frac{\cos^3\theta}{r} + O(r^{-2}) \quad \sigma_{22} = \frac{2p_o}{\pi h}\frac{\sin^2\theta\cos\theta}{r} \\ &\qquad + O(r), \\ \sigma_{12} &= \frac{2p_o}{\pi h}\frac{\sin\theta\cos^2\theta}{r} + O(r^{-2}) \text{ as } r \to \infty; \end{aligned} \tag{1.14}$$

further, the intermediate approximate solution coincides with Melan's even within terms of order $O(r^{-2})$ as $r \to \infty$.

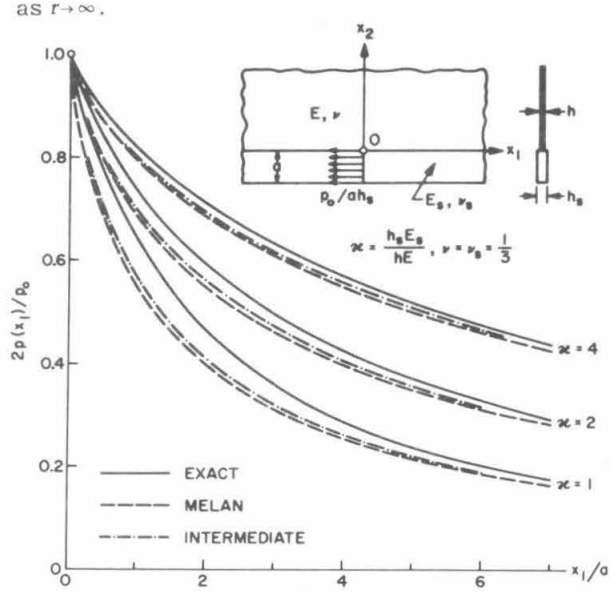

FIG. 2 MELAN'S SECOND PROBLEM. DECAY OF THE AXIAL STIFFENER-FORCE FOR A RECTANGULAR STIFFENER

[1] See, for example, Girkmann [8], art. 31.

[2] See [1] for the corresponding results.

[3] A related two-dimensional solution is due to Bufler [9], who considered a *concentrated* tangential load applied at a point of the free edge of the stiffener. In [2] the loading is idealized by body forces *uniformly distributed* over a stiffener cross section.

[4] Note that the direction of the load in [2] is opposite to that chosen here.

In contrast, the sheet stresses in the vicinity of the applied stringer-load, i.e., *near the origin*, are quite sensitive to the underlying choice of the stringer model. In this connection we cite from [2] the subsequent asymptotic results. For the *exact solution*,

$$\sigma_{11} = \frac{p_o}{4\pi\,\gamma ah}\,[(3+\beta)\,(\pi-2\theta)-2\,\sin 2\theta\,]+o(1),$$

$$\sigma_{22} = \frac{p_o}{4\pi\,\gamma ah}\,[(1-\beta)\,(\pi-2\theta)+2\,\sin 2\theta]+o(1),$$

$$\sigma_{12} = \frac{-p_o}{2\pi\,\gamma ah}\,[(1+\beta)\log r]+O(1)\ \text{as}\ r\to 0, \tag{1.15}$$

in which

$$\gamma = \frac{4}{1+\nu}+(3-\nu)\left[\frac{\kappa}{1+\nu_s}-\frac{1}{1+\nu}\right],$$

$$\beta = \frac{(1-3\nu_s)\gamma}{4+(1+\nu)\,\kappa-(1+\nu_s)}\,. \tag{1.16}$$

For the *intermediate approximate solution*,

$$\sigma_{11} = \frac{p_o}{2\pi\kappa\,(3-\nu)ah}\left[\frac{3+\nu}{1+\nu}\,(\pi-2\theta)-\sin 2\theta\right]+o(1),$$

$$\sigma_{22} = \frac{-p_o}{2\pi\kappa\,(3-\nu)ah}\left[\frac{1-\nu}{1+\nu}\,(\pi-2\theta)-\sin 2\theta\right]+o(1),$$

$$\sigma_{12} = \frac{-2p_o}{\pi\kappa(1+\nu)\,(3-\nu)\,ah}\log r+O(1)\ \text{as}\ r\to 0\,. \tag{1.17}$$

Finally, for *Melan's solution*,

$$\sigma_{11} = \frac{p_o}{2\pi\kappa ah}\left[\pi-2\theta-\frac{1}{2}\,\sin 2\theta\,\right]+o(1),$$

$$\sigma_{22} = \frac{p_o}{4\pi\kappa ah}\,\sin 2\theta+o(1), \tag{1.18}$$

$$\sigma_{12} = \frac{-p_o}{2\pi\kappa ah}\,\log r+O(1)\ \text{as}\ r\to 0\,.$$

[1] See, for example Girkmann [8], p. 68.

It is of interest to compare the singular behavior of $\sigma_{\alpha\beta}$ at $r = 0$ displayed in (1.15), (1.17), (1.18) with that inherent in the classical generalized plane-stress solution[1] for a semi-infinite sheet of thickness h (occupying the present sheet-domain) under a concentrated tangential edge-load of magnitude p_o applied at the origin in the negative x_1-direction. The latter solution furnishes the stress field

$$\sigma_{11} = \frac{2p_o}{\pi h}\,\frac{\cos^3\theta}{r},\quad \sigma_{22} = \frac{2p_o}{\pi h}\,\frac{\sin^2\theta\cos\theta}{r},$$

$$\sigma_{12} = \frac{2p_o}{\pi h}\,\frac{\sin\theta\cos^2\theta}{r}\,. \tag{1.19}$$

Thus, while all sheet stresses $\sigma_{\alpha\beta}$ induced by the *direct* application of the load, according to (1.19), become unbounded as r^{-1} at the point of load application, the normal stresses σ_{11}, σ_{22} remain finite as $r\to 0$ when the load is transferred to the sheet by means of a stiffener, for the three stiffener models under discussion; moreover, the shear stress σ_{12} –though unbounded at the origin – now exhibits merely a logarithmic singularity. These conclusions reflect the beneficial mitigating effect of the edge-stiffener. In contrast, the introduction of the stiffener has no significant influence upon the far-field behavior of the sheet stresses: σ_{11}, σ_{22}, σ_{12} in (1.19) coincides with the corresponding dominating terms in (1.14) of order $O(r^{-1})$ as $r\to\infty$.

The stresses σ_{11}, σ_{22} in (1.15), (1.17), (1.18), while finite, are discontinuous at $r = 0$. Although the limiting values of these stresses as $r\to 0$ along a fixed ray of approach exist, they are different in all three instances. Also, whereas the *order* of the singularity of σ_{12} at the origin is logarithmic in (1.15), (1.17), and (1.18), its *detailed character* (strength) depends on the particular choice of the stiffener model. For the preceding reasons Melan's solution, the intermediate approximation, and the exact two-dimensional solution lead to substantially different sheet stresses in the vicinity of the load. This state of affairs is illustrated by Fig. 3, which shows the results obtained for σ_{11} along the interface between sheet and stringer. As is evident from the figure, the discrepancies near the load between the three solutions depicted here diminish with increasing values of the stiffness-ratio κ. Regardless of the value of κ, however, the three sets of curves in Fig. 3 are in close agreement for sufficiently large x_1/a because of (1.14).

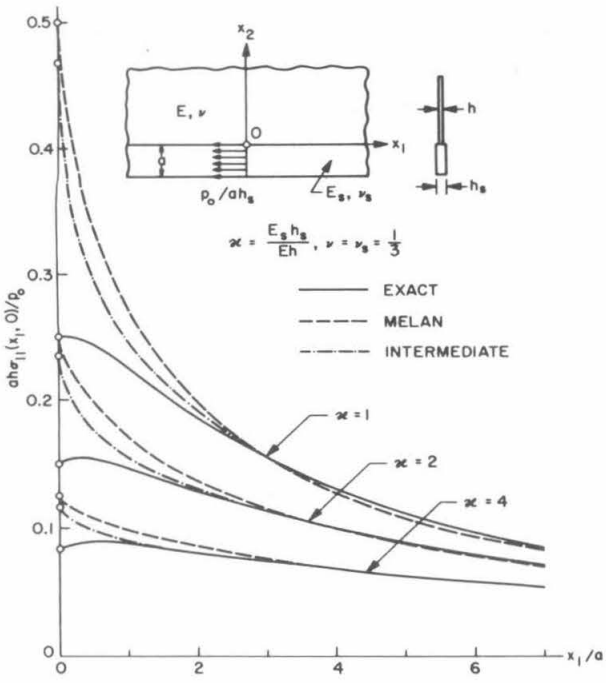

FIG. 3 MELAN'S SECOND PROBLEM. SHEET STRESS σ_{11} AT INTERFACE FOR A RECTANGULAR STIFFENER

The modification of Melan's first problem arising if the stringer, instead of being continuously attached, is fastened to the sheet by means of an evenly spaced array of rigid rivets, was investigated by Budiansky and Wu [10]. Fisher [11] dealt with the counterpart of the first problem for a circular cylindrical shell that is reinforced by one or more axial stiffeners.

Generalizations of Melan's problems to semi-infinite or finite stringers and to other sheet-stringer configurations have been considered by various authors and diverse analytical methods.[1] Among these studies we single out a paper by Koiter [12], who used a Mellin-transform technique to deduce a solution, exact within Melan's simplifying assumptions, of Melan's problems for a semi-infinite stringer. The more complicated problem occasioned by the diffusion of an axial load from a transverse stringer, a finite segment of which overlaps with, and is continuously bonded to, a semi-infinite sheet, was posed first by Reissner [13] and will be discussed in Section 3. Meanwhile we turn to a class of plane load-transfer problems which apart from its general interest has a particular bearing on Reissner's problem.

2. LOAD-TRANSFER BETWEEN OVERLAPPING BONDED ELASTIC SHEETS

We are concerned here with the load-exchange between two partly overlapping and continuously bonded finite sheets of uniform thickness and not necessarily the same elastic properties, which are in equilibrium under a given in-plane loading that is confined to the unattached portions of the sheet edges (Fig. 4). What follows is a condensed and clarified version of [3].

As indicated in Fig. 4, let the two sheets be designated by S' and S'', respectively, calling D', h' and D'', h'' the corresponding sheet-domains and sheet-thicknesses. Next, let D be the domain of adhesion, i.e., the intersection of D' with D'', denoting by D'_* and D''_* the respective unattached subregions of D' and D'' (free sheet-domains). Further, let C', C'' and C'_*, C''_* stand for the bonded and the free segments of the boundaries of D' and D''. Finally, call G', G'' and ν', ν'' the shear moduli and Poisson-ratios of S' and S''. We aim at the determination of the deformations and stresses in either sheet within the conventional theory of generalized plane stress. Such a two-dimensional treatment of the problem is of course useful only if h' and h'' are both appropriately small compared to the characteristic dimensions of the sheet-faces. Moreover, with reference to the side-views (a) and (b) in Fig. 4, we note that the symmetric mode of attachment (b) renders the present analysis more realistic since it tends to minimize bending effects that are being left out of account.

Choose rectangular cartesian coordinates (x_1, x_2) in a plane parallel to the sheet-faces and write[2] u'_α, $\sigma'_{\alpha\beta}$ and u''_α, $\sigma''_{\alpha\beta}$ for the corresponding component fields of displacement and stress[3] in S' and S'', respectively. The pertinent *stress equations of equilibrium* now take the form

$$\sigma'_{\alpha\beta,\,\beta} = 0 \text{ on } D'_*, \quad \sigma'_{\alpha\beta,\,\beta} - \frac{f_\alpha}{h'} = 0 \text{ on } D,$$
$$\sigma''_{\alpha\beta,\,\beta} = 0 \text{ on } D''_*, \quad \sigma''_{\alpha\beta,\,\beta} + \frac{f_\alpha}{h''} = 0 \text{ on } D, \tag{2.1}$$

provided f_α represents the surface-density components of the "interior bond-forces" exerted by S'

[1] See [2], [4] for references.

[2] Greek subscripts hereafter are understood to have the range (1, 2) and the usual indicial notation is employed.

[3] For brevity the terms "displacement" and "stress" are used synonymously with "thickness average of displacement" and "thickness average of stress."

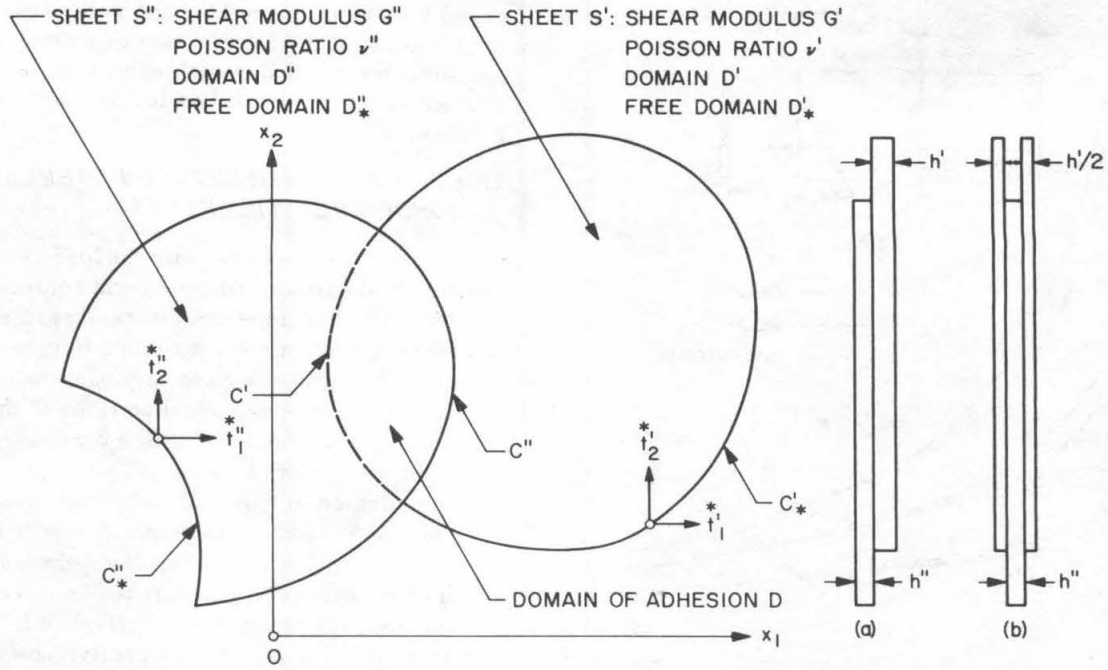

FIG. 4 GEOMETRY OF OVERLAPPING BONDED SHEETS

upon S'' over the domain of adhesion D. These interior bond-forces enter (2.1) in the role of reactive body forces and are among the unknowns of the problem. The *stress-displacement relations*, in turn, furnish

$$\sigma'_{\alpha\beta} = 2G'\left[u'_{(\alpha,\beta)} + \frac{\nu'}{1-\nu'}\,\delta_{\alpha\beta}\,u'_{\gamma,\gamma}\right] \text{ on } D'_* \text{ and } D,$$

$$\sigma''_{\alpha\beta} = 2G''\left[u''_{(\alpha,\beta)} + \frac{\nu''}{1-\nu''}\,\delta_{\alpha\beta}\,u''_{\gamma,\gamma}\right] \text{ on } D''_* \text{ and } D, \tag{2.2}$$

where $\delta_{\alpha\beta}$ is the Kronecker-delta.

To the field equations (2.1), (2.2) one needs to adjoin the *bond conditions*

$$u'_\alpha = u''_\alpha \text{ on } D, \tag{2.3}$$

as well as the *boundary conditions*

$$\sigma'_{\alpha\beta}n_\beta = \overset{*}{t}{}'_\alpha \text{ on } C'_*, \quad \sigma''_{\alpha\beta}n_\beta = \overset{*}{t}{}''_\alpha \text{ on } C''_*, \tag{2.4}$$

in which n_β are the components of the unit outward normal vector of the sheet-edges, while $\overset{*}{t}{}'_\alpha$ and $\overset{*}{t}{}''_\alpha$ are the components of the given edge tractions, applied along C'_* and C''_*, respectively. In addition, the requirement that the displacements in either sheet be continuous, together with elementary equilibrium considerations, leads to the *transition conditions*

$$\overset{+}{u}{}''_\alpha = \bar{u}''_\alpha, \quad h''\overset{+}{\sigma}{}''_{\alpha\beta}n_\beta = (h'\bar{\sigma}'_{\alpha\beta} + h''\bar{\sigma}''_{\alpha\beta})n_\beta \text{ on } C',$$

$$\overset{+}{u}{}'_\alpha = \bar{u}'_\alpha, \quad h'\overset{+}{\sigma}{}'_{\alpha\beta}n_\beta = (h'\bar{\sigma}'_{\alpha\beta} + h''\bar{\sigma}''_{\alpha\beta})n_\beta \text{ on } C'', \tag{2.5}$$

Here $\overset{+}{u}{}''_\alpha$, $\overset{+}{\sigma}{}''_{\alpha\beta}$ and $\bar{u}''_\alpha$, $\bar{\sigma}''_{\alpha\beta}$ denote the respective limits of u''_α, $\sigma''_{\alpha\beta}$ as the arc C' is approached from the free sheet-domain D''_* or from the domain of adhesion D; the symbols $\overset{+}{u}{}'_\alpha$, $\overset{+}{\sigma}{}'_{\alpha\beta}$ and $\bar{u}'_\alpha$, $\bar{\sigma}'_{\alpha\beta}$ are to be interpreted analogously.

The two-dimensional boundary-value problem governed by the field equations (2.1), (2.2), in conjunction with conditions (2.3), (2.4), (2.5), is not a standard problem in the theory of generalized plane stress. One is therefore entitled to ask whether this problem is in fact well posed. We now make clear that the foregoing question is not merely rhetorical. The tractions on the bonded edge-segments of S' and S'' evidently obey

$$t'_\alpha = \sigma'_{\alpha\beta}n_\beta \text{ on } C', \quad t''_\alpha = \sigma''_{\alpha\beta}n_\beta \text{ on } C''. \tag{2.6}$$

Since the arcs C' and C'' are, by hypothesis, free of *applied* tractions, one may at first sight expect that (2.6), with t'_α and t''_α replaced by zero, are boundary conditions to be imposed alongside (2.4). Such an a priori assignment, however, gives rise to an overdeterminate problem and is inadmissible within the current two-dimensional treatment of the original load-transfer problem under consideration. Indeed, the tractions t'_α and t''_α in (2.6) are reactive in character – they represent the *edge bond-tractions* exerted by the two sheets upon each other and accompany the *interior bond-tractions* encountered earlier. The self-consistency of the preceding two-dimensional formulation of the problem follows from its reduction to a standard inclusion problem to which we turn presently.

Bearing in mind (2.3), set

$$u_\alpha = u'_\alpha = u''_\alpha,\quad \sigma_{\alpha\beta} = \frac{1}{h}(h'\sigma'_{\alpha\beta} + h''\sigma''_{\alpha\beta}) \text{ on } D,\ h = h' + h'' \tag{2.7}$$

and introduce the fictitious elastic constants

$$G = \frac{1}{h}(h'G' + h''G''),\quad \nu = \frac{\nu'(1-\nu'') + \nu''(1-\nu')\rho}{1-\nu'' + (1-\nu')\rho}, \tag{2.8}$$

where ρ is the stiffness-ratio defined by

$$\rho = \frac{h''G''}{h'G'}. \tag{2.9}$$

Then (2.1), (2.2) at once give

$$\sigma_{\alpha\beta,\beta} = 0,\quad \sigma_{\alpha\beta} = 2G\left[u_{(\alpha,\beta)} + \frac{\nu}{1-\nu}\,\delta_{\alpha\beta}u_{\gamma,\gamma}\right] \text{ on } D \tag{2.10}$$

and (2.5) become

$$u_\alpha = \overset{+}{u}{}''_\alpha,\quad h\sigma_{\alpha\beta}n_\beta = h''\overset{+}{\sigma}{}''_{\alpha\beta}n_\beta \text{ on } C',$$
$$u_\alpha = \overset{+}{u}{}'_\alpha,\quad h\sigma_{\alpha\beta}n_\beta = h'\overset{+}{\sigma}{}'_{\alpha\beta}n_\beta \text{ on } C''. \tag{2.11}$$

Consider now (2.10) together with those field equations among (2.1), (2.2) that pertain to the free sheet-domains D'_*, D''_*, subject to the boundary conditions (2.4) and the transition conditions (2.11). This system of equations clearly characterizes $u_\alpha, \sigma_{\alpha\beta}$ on D, $u'_\alpha, \sigma'_{\alpha\beta}$ on D'_*, and $u''_\alpha, \sigma''_{\alpha\beta}$ on D''_* as the solution to an ordinary second boundary-value problem of generalized plane stress for a composite body: it governs the displacements and stresses in *three* sheets that occupy the domains D, D'_*, and D''_*, respectively, are continuously bonded along the common edges C', C'', and are in equilibrium under the edge tractions $\overset{*}{t}{}'_\alpha$, $\overset{*}{t}{}''_\alpha$ applied to C'_* C''_*; further, the thickness and the elastic constants of the "inclusion" occupying D are h and G, ν, whereas the two outside sheets have the same thickness and elastic properties as S' and S'', respectively.

Once the inclusion problem has been solved, the displacements and stresses in the original load-transfer problem are known throughout the free sheet-domains, as are the displacements within the domain of adhesion. Moreover, the stresses and interior bond-forces acting on the overlapping portions of S' and S'' are now directly computable from the stress field prevailing in the inclusion. Equations (2.10), (2.2), by virtue of (2.7) to (2.9), furnish

$$\sigma'_{\alpha\beta} = \frac{G'}{G}(\sigma_{\alpha\beta} + \rho\eta\delta_{\alpha\beta}\sigma_{\gamma\gamma}) \text{ on } D, \tag{2.12}$$
$$\sigma''_{\alpha\beta} = \frac{G''}{G}(\sigma_{\alpha\beta} - \eta\delta_{\alpha\beta}\sigma_{\gamma\gamma}) \text{ on } D,$$

$$f_\alpha = \frac{\rho\eta h}{1+\rho}\sigma_{\gamma\gamma,\alpha} \text{ on } D, \tag{2.13}$$

provided

$$\eta = \frac{\nu' - \nu''}{(1+\nu')(1-\nu'') + (1+\nu'')(1-\nu')\rho}. \tag{2.14}$$

Since the inclusion problem to which we have been led is well posed,[1] the same is true of the original problem.

It is of interest to examine how the total force transmitted by S' to S'' is apportioned among the interior and the edge bond-forces acting on S''. To this end we adopt the notation

$$R_\alpha = h'\int_{C'_*} \overset{*}{t}{}'_\alpha ds,\quad F_\alpha = \int_D f_\alpha dA,$$
$$P_\alpha = h''\int_{C''} \sigma''_{\alpha\beta}n_\beta ds,\quad Q_\alpha = -h'\int_{C'} \sigma'_{\alpha\beta}n_\beta ds, \tag{2.15}$$

so that R_α, F_α, P_α, and Q_α, in this order, refer to the

[1] See [3] for details.

components of the resultant external load applied to S', the resultant interior bond-force upon S'', the resultant edge bond-force exerted on S'' along C'', and its counterpart along C'. Then, in view of the equilibrium of the sheet S',

$$P_\alpha + Q_\alpha + F_\alpha = R_\alpha \tag{2.16}$$

and, as shown in [3],

$$P_\alpha = \frac{\rho}{1+\rho} R_\alpha - \frac{\rho\eta h'}{1+2\rho\eta} \int_{C''} \bar{\sigma}'_{\gamma\gamma} n_\alpha ds$$

$$Q_\alpha = \frac{1}{1+\rho} R_\alpha - \frac{\rho\eta h'}{1+2\rho\eta} \int_{C'} \bar{\sigma}'_{\gamma\gamma} n_\alpha ds. \tag{2.17}$$

The particular case in which the two sheets S' and S'' have the same Poisson-ratio – though possibly different shear moduli – merits separate attention. In this instance $\nu' = \nu''$ and thus $\eta = 0$ according to (2.14). Consequently, from (2.13), (2.15), (2.17),

$$f_\alpha = 0 \text{ on } D\,, \quad F_\alpha = 0\,, \quad P_\alpha = \frac{\rho}{1+\rho} R_\alpha, \quad Q_\alpha = \frac{1}{1+\rho} R_\alpha\,. \tag{2.18}$$

Equations (2.18) reaffirm results previously deduced by Goodier and Hsu [14], who limited their discussion to the special case at hand. The first of (2.18) expresses the somewhat startling conclusion that the interior bond-forces vanish identically when $\nu' = \nu''$, the entire load-transmission being effected by the edge bond-tractions. It should be recognized, however, that this conclusion – as indeed the very emergence of edge bond-tractions – reflects a degeneracy inherent in the present two-dimensional treatment of the problem. A *three*-dimensional solution of this problem would inevitably involve merely *interior* bond-forces, which, for $\nu' = \nu''$, are apt to be predominately confined to a boundary layer adjacent to the perimeter of the domain of adhesion.

The inclusion analogy at which we have arrived, apart from its theoretical significance, is useful on several grounds: first, it reduces the original problem to one which, although in general singular, is within the reach of the methods of integration available in two-dimensional elastostatics; second, it enables one to reinterpret known solutions of inclusion problems as solutions of associated adhesion problems; further, the analogy is of some interest in connection with experimental stress analysis.

The extension of the inclusion analogy to unbounded sheet-domains is easily achieved. Nor is there any essential complication inherent in admitting the possibility that bond occurs only over subregions of the overlapping sheet portions. Next, as to the loading, it is a simple matter to accommodate applied body forces, in addition to edge loads. Finally, the generalization of this reduction scheme to multiply layered bonded sheet assemblies offer no difficulties.

In [3] the appropriate adaptation of the inclusion analogy was applied to the load-transfer occurring between two semi-infinite sheets that are mutually attached throughout an overlapping strip parallel and adjacent to the two sheet edges. The loading was initially assumed to consist of a single concentrated force applied to one of the sheets (within the corresponding free sheet-domain) at right angles to the strip of adhesion. This problem was chosen because of its comparative simplicity and since it has a bearing on the stress analysis of lap joints. The associated reduced problem was solved with the aid of Airy's stress function and the exponential Fourier transform. The practical significance of the fundamental singular solution thus obtained stems from the fact that, in conjunction with the principle of superposition, it disposes of essentially arbitrary

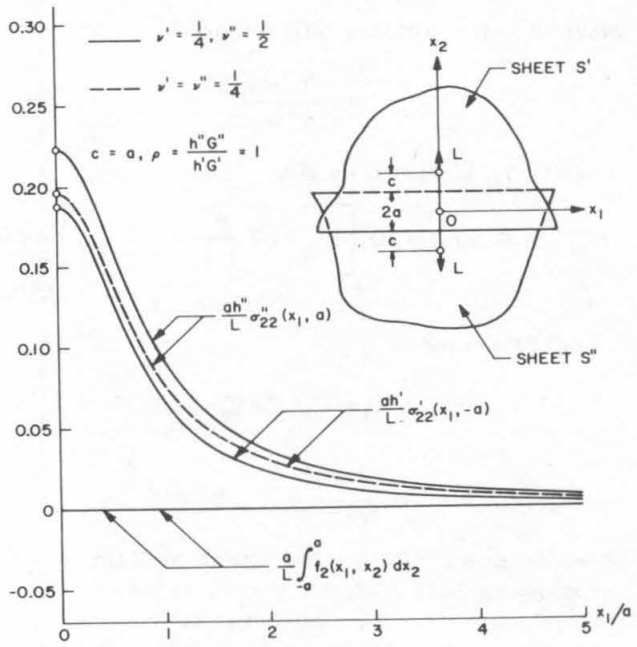

FIG. 5 OVERLAPPING BONDED SEMI-INFINITE SHEETS. COMPARISON OF INTERIOR AND EDGE BOND-FORCES

loads applied to either free sheet portion perpendicular to the sheet edges. If the loading is self-equilibrated, the problem represents a sensible idealization of physically realizable circumstances involving two sheets of sufficiently large but finite extent.

We reproduce here, in Fig. 5, only results pertaining to the comparative size of the interior and edge bond-forces per unit width of the strip of adhesion for the special case of two equal, opposite, and collinear concentrated loads. The dashed curve refers to $\rho = 1$ and $\nu' = \nu'' = \frac{1}{4}$: it represents the lineal intensity of the edge bond-forces at *either* edge in view of the prevailing geometric, material, and load symmetry.[1] The corresponding interior bond-forces vanish identically, as predicted by the first of (2.18). The solid curves are based on $\rho = 1$ and $\nu' = \frac{1}{4}$, $\nu'' = \frac{1}{2}$. For such a choice of the parameters the edge bond-tractions exerted on S'' are somewhat larger than those acting on S', but the lineal intensity of the interior bond-forces, while no longer zero, remains indistinguishable from zero on the scale of Fig. 5. This conclusion suggests that the influence of the interior bond-forces upon the mechanism of load-transfer is relatively unimportant even if the two bonded sheets fail to have the same Poisson ratio.

3. LOAD-DIFFUSION FROM A TENSION-BAR INTO A SEMI-INFINITE SHEET

Our next objective is to deal with the diffusion of an axial load from a stringer that is perpendicular to the straight edge of a semi-infinite sheet and a finite segment which is continuously bonded to the sheet. The geometry of this sheet-stringer assembly is illustrated in Fig. 6. We call ℓ the length of the overlapping stringer segment and otherwise employ the same notation as in Section 1. In particular, for the special case of a rectangular stringer cross section (see (*b*) in Fig. 6), the thickness and width of the latter are designated by h_s and a, respectively. The foregoing load-transfer problem was initially posed by Reissner [13], who adhered strictly to the assumptions underlying Melan's treatment of his first problem.[2] Reissner's formulation thus includes the one-dimensional stringer equations

$$\frac{p(x)}{A} = \sigma(x) = E_s \epsilon(x) \ , \ p'(x) + q(x) = 0 \ (0 < x < \ell) \quad (3.1)$$

[1] Observe that $\rho = 1$, in particular for $h' = h''$ and $G' = G''$.

[2] See assumptions (i) through (iv) in Section 1. A sketch of the rather elaborate subsequent history of Reissner's problem may be found in [4].

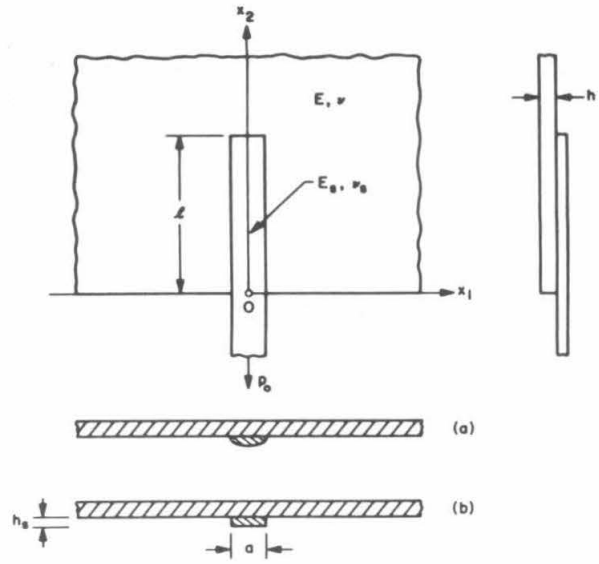

FIG. 6 GEOMETRY OF REISSNER'S PROBLEM

which take the place of (1.2), (1.3) in Melan's problems. Evidently, $p(x)$, $\sigma(x)$, $\epsilon(x)$, and $q(x)$ here refer to the axial scalar stringer-force, the corresponding stress and strain, and the scalar bond-force per unit length exerted on the stringer – all evaluated at $x_2 = x$. On combining (3.1) with the kinematic bond condition resulting from the hypothesis of ideal line-contact between sheet and stringer, one arrives at

$$\frac{p(x)}{AE_s} = [p_o - p(0)]\, \mathring{\epsilon}(x,0) + p(\ell)\, \mathring{\epsilon}(x,\ell) - \int_0^\ell p'(\xi)\, \mathring{\epsilon}(x,\xi)\, d\xi \quad (0 < x < \ell) \ , \quad (3.2)$$

where p_o is once again the magnitude of the applied load, while $\mathring{\epsilon}(x,\xi)$ is the thickness-average of the extensional strain parallel to the x_2-axis at $(0,x)$, due to a unit concentrated load applied at $(0,\xi)$ in the negative x_2-direction. This influence function, according to Melan's [15] generalized plane-stress solution for the half-plane under an internal concentrated load admits the elementary representation

$$\mathring{\epsilon}(x,\xi) = \frac{(3-\nu)(1+\nu)}{4\pi hE} \frac{1}{x-\xi} + \mathring{R}(x,\xi) \ ,$$

$$\mathring{R}(x,\xi) = \frac{1}{4\pi hE}\left[\frac{8-(3-\nu)(1+\nu)}{x+\xi} + \frac{2(1+\nu)^2\,\xi(x-\xi)}{(x+\xi)^3}\right] \ , \quad (0 \le x \le \ell, \ 0 \le \xi \le \ell, \ x \ne \xi) \ . \quad (3.3)$$

Consequently, $\mathring{\epsilon}(x, \xi)$ has a singularity of the Cauchy type[1] at $x=\xi$; the "regular part" $\mathring{R}(x, \xi)$ of $\mathring{\epsilon}(x, \xi)$, though continuous for $0<x\leq\ell$, $0<\xi\leq\ell$, is unbounded at the origin of the (x,ξ)-plane.

The leading two terms in (3.2) allow for the eventuality that portions of the applied stringer-load p_o are communicated to the sheet through bond-forces concentrated at the ends of the attached stringer segment: in fact, $p_o-p(0)$ is evidently the magnitude of the concentrated bond-force at $x_2=0$, while $p(\ell)$ is the load-portion transferred to the sheet abruptly at the end of the stringer, $x_2=\ell$. Reissner [13] argued on physical grounds that such singular load-transfer cannot occur within the line-contact model for the stringer attachment and was thus led to accompany (3.2) by the boundary conditions

$$p(0)=p_o\ ,\ p(\ell)=0. \tag{3.4}$$

The question as to whether or not concentrated bond-forces actually arise within the above treatment of the problem has been the subject of some controversy in the literature.[2] Clearly, this is an issue that ought to be decided by the solution of the problem, rather than one that should need to be settled in advance. It was shown in [4], by means of a minor generalization of a scheme due to Muskhelisvili [16], that (3.2) – under rather mild and physically plausible regularity assumptions regarding the unknown function p – *implies* (3.4). This proof constitutes an analytical confirmation of Reissner's conjecture.

Equations (3.4) reduce (3.2) to

$$\frac{p(x)}{AE_s}+\int_0^{\ell} p'(\xi)\,\mathring{\epsilon}(x,\xi)\,d\xi=0\ (0<x<\ell)\ , \tag{3.5}$$

which is a singular integro-differential equation for the desired stringer-force distribution, analogous to (1.7) and alike in structure to Prandtl's equation for the aerodynamic load distribution on a wing of finite span.

Equation (3.5), in contrast to (1.7), does not yield to a direct explicit solution because of its finite range of integration and in view of the greater complexity of its kernel, which is no longer of the translation type. It is possible, however, to transform (3.5) into an integral equation of Fredholm's third kind that is amenable to a numerical solution. An investigation aiming at this objective is currently in progress. We still cite here asymptotic estimates for the derivative of the stringer-force at the ends of the attachment, which were deduced from (3.5) in [4] by a scheme similar to the one employed in the proof of (3.4):

$$p'(x)=O(x^{-\alpha_*}) \text{ as } x\to 0\ ,\ p'(x)=O(1/\sqrt{\ell-x}) \text{ as } x\to\ell\ , \tag{3.6}$$

where α_* is the unique real root on the interval (0, 1) of the transcendental equation

$$\cos[(1-\alpha)\pi]-\frac{2(1+\nu)}{3-\nu}(1-\alpha)^2+\frac{8-(3-\nu)(1+\nu)}{(3-\nu)(1+\nu)}=0\ \left(0<\nu<\frac{1}{2}\right). \tag{3.7}$$

The graph of α_* as a function of the Poisson-ratio of the sheet is displayed in Fig. 7, according to which the singularity of $p'(x)$ at $x=0$ becomes steadily more severe with increasing values of ν. The estimates (3.6), because of the last of (3.1), at the same time characterize the singular behavior of the bond-force density $q(x)$ as $x\to 0$ and $x\to\ell$. The first of (3.6) agrees with a conclusion reached by Hens [17], who used a Mellin-transform technique in dealing with the limiting case of Reissner's problem for a semi-infinite stringer. On the other hand, as is to be anticipated, the second of (3.6) conforms to Koiter's [12] conclusion regarding the singularity of

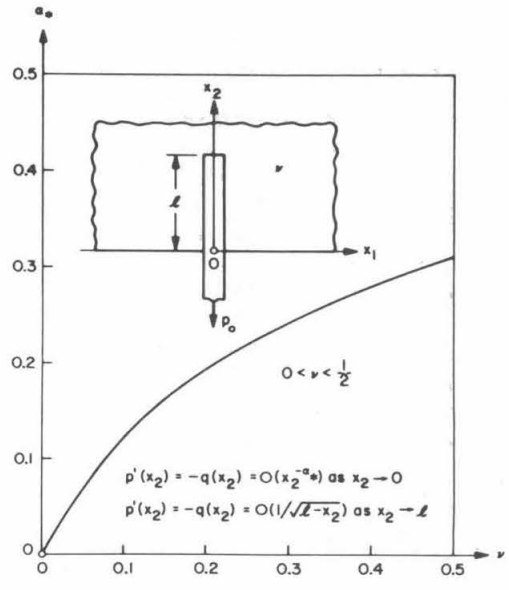

FIG. 7 REISSNER'S PROBLEM. LINE-CONTACT MODEL. DEPENDENCE OF α_* ON POISSON'S RATIO

[1] The integral in (3.2) needs to be interpreted in the sense of its principal value.

[2] See [4] for references.

p' at the end of the bar in Melan's first problem for a semi-infinite stringer.

All of the preceding considerations apply to a stringer of arbitrary cross-sectional shape. If, in particular, the cross section is rectangular (see Fig. 6b) with h_s/a and h/a small enough, Reissner's problem may sensibly be viewed as one in the theory of overlapping bonded sheets discussed in Section 2. Unforunately, the associated reduced problem to which the inclusion analogy gives rise in this instance is highly singular and of formidable complexity.

An attempt to combine Reissner's formulation with the theory of overlapping sheets is due to Goodier and Hsu [14], who presupposed a rectangular stringer cross section and noted that for $\nu_s=\nu$, (2.18) predicts a resultant edge bond-force, supplied to the sheet at its boundary, of magnitude

$$p_o-p(0)=\frac{1}{1+\kappa}\,p_o\ ,\quad \kappa=\frac{h_sE_s}{hE}. \tag{3.8}$$

Guided by (3.8), the first of the boundary conditions (3.4) is in [14] replaced by

$$p(0)=\frac{\kappa}{1+\kappa}\,p_o\ , \tag{3.9}$$

while the integro-differential equation (3.2) is retained.[1] It is clear from our earlier discussion of (3.4) that the ad hoc assignment (3.9) of $p(0)$ is incompatible with (3.2). If edge bond-forces concentrated at the ends of the attached stringer segment are to be admitted, the hypothesis of *line-contact* underlying Reissner's idealization of the problem needs to be relinquished in favor of a suitable *area-contact* model for the stringer attachment. Such an alternative approximate treatment of Reissner's problem, originally proposed by Krahn [18], was carried out in [4] and is summarized below.

For the present purpose we return once again to a stringer of arbitrary uniform cross section, retain the one-dimensional characterization (3.1) of the stringer, but now regard the latter fastened to the sheet throughout a strip of finite constant width[2] $a>0$, which is symmetric about the x_2-axis. Further, we assume the bond-forces to be uniformly distributed across the width of this strip and, as a kinematic bond condition, adopt the requirement that the axial stringer strain at each cross section match the corresponding sheet strain averaged over the width of the strip of adhesion. Under the preceding assumptions (3.2) gives way to

$$\frac{p(x)}{AE_s}=[p_o-p(0)]\,\hat{\epsilon}\,(x,0)+p(\ell)\,\hat{\epsilon}(x,\ell) - \int_0^{\ell} p'(\xi)\hat{\epsilon}(x,\xi)\,d\xi\ \ (0<x<\ell)\ , \tag{3.10}$$

provided $\hat{\epsilon}(x,\xi)$ stands for the appropriate average extensional sheet strain at $x_2=x$ due to a load of unit magnitude applied in the negative x_2-direction, this loading being uniformly distributed over a straight-line segment of length a that is centered at $(0,\xi)$ and parallel to the x_1-axis.

An elementary closed representation for $\hat{\epsilon}$ is readily deduced[3] from Melan's [15] basic singular generalized plane-stress solution for the half-plane. We indicate here merely the structure of this influence function, which is of the form

$$\hat{\epsilon}(x,\xi)=\frac{1-\nu^2}{2ahE}\ \mathrm{sgn}\,(x-\xi) +R(x,\xi)\ (0\le x\le\ell,\ 0\le\xi\le\ell,\ x\neq\xi)\ , \tag{3.11}$$

where sgn stands for the signum-function,[4] while $R(x,\xi)$ is an elementary function continuous for $0\le x\le\ell$, $0\le\xi\le\ell$ and continuously differentiable for $0\le x\le\ell$, $0\le\xi\le\ell$, $x\neq\xi$. Hence $\hat{\epsilon}(x,\xi)$, unlike $\mathring{\epsilon}(x,\xi)$ of (3.3), has only a finite jump discontinuity at $x=\xi$. From (3.11) follows

$$\hat{\epsilon}(x,x-)-\hat{\epsilon}(x,x+)=\frac{1-\nu^2}{ahE}\ . \tag{3.12}$$

The mild singular behavior of $\hat{\epsilon}$, as compared to $\mathring{\epsilon}$, renders (3.10) more easily tractable than (3.2). Indeed, an integration by parts applied to (3.10), with proper attention to (3.12), carries this integro-differential equation into the integral equation of Fredholm's second kind

$$\left[\frac{1}{AE_s}+\frac{1-\nu^2}{ahE}\right]p(x)-\int_0^{\ell}p(\xi)K(x,\xi)\,d\xi =p_o\,\hat{\epsilon}(x,0)\ (0\le x\le\ell)\ . \tag{3.13}$$

[1] The numerical solution of (3.2) reported in [14] involves the additional assumption that $p(\ell)=p(0.9\ell)$, which takes the place of the second of (3.4).

[2] For a fully bonded stringer of rectangular cross section (Fig. 6), a coincides with the width of the cross section.

[3] See Section 1 of [4].

[4] $\mathrm{sgn}(x)=1\ (0<x<\infty)$, $\mathrm{sgn}\,(x)=-1\ (-\infty<x<0)$.

The kernel K in (3.13) has the structure[1]

$$K(x,\xi)\equiv\frac{\partial}{\partial\xi}\hat{\epsilon}(x,\xi)=-\frac{1}{2\pi a^2 hE}$$

$$\left[(1+\nu)(1-3\nu)\log\frac{|x-\xi|}{a}-(1-2\nu+5\nu^2)\log\frac{x+\xi}{a}\right]$$

$$+M(x,\xi) \qquad (3.14)$$

in which $M(x,\xi)$ is continuous for $0<x\leq\ell$, $0<\xi\leq\ell$ and tends to a finite limit as the origin of the (x,ξ) -plane is approached along a ray of fixed direction. Also, $\hat{\epsilon}(x,0)$ is continuous for $0\leq x\leq\ell$. These observations account for the *closed* range of validity of the Fredholm equation (3.13), whose kernel – though singular – is integrable in the ordinary sense. The numerical solution of (3.13) presents no particular difficulties.

It is essential to emphasize that (3.13) determines the desired stringer-force $p(x)$ over the *entire* range $0\leq x\leq\ell$. Advance assignments of the end-values $p(0)$ and $p(\ell)$, which govern the load portions transmitted to the sheet through bond-forces concentrated at the ends of the attachment, are neither necessary nor – if made arbitrarily – consistent with (3.13). The asymptotic behavior of $p'(x)$, and thus of $q(x)$, as $x\to0$ and $x\to\ell$, may be extracted[2] from (3.10). One finds that

$$p'(x)=-16\nu c[p_o-p(0)]\log(x/\ell)+O(1)\ \text{as}\ x\to0\ ,$$

$$p'(x)=2(1+\nu)(1-3\nu)cp(\ell)\log[(\ell-x)/\ell]+O(1)\ \text{as}\ x\to\ell, \qquad (3.15)$$

where

$$c=\frac{AhE_s}{4\pi ah[ahE+(1-\nu^2)AE_s]}\ . \qquad (3.16)$$

Since (3.4) does not hold true for the area-contact model,[3] (3.15) predicts that $p'(x)\to+\infty$ logarithmically as $x\to0$, i.e., at the edge of the sheet, unless $\nu=0$; similarly, $p'(x)$ has a logarithmic singularity[4] at the end of the stringer unless $\nu=1/3$.

One would expect the solution for $p(x)$ based on (3.13) to approach that furnished by (3.2) in the limit as $a\to0$. It appears to be quite difficult, however, to confirm analytically this transition to the solution supplied by the line-contact model.

A variant of the preceding area-contact treatment of Reissner's problem was introduced by LeFevre, Mudge, and Dickie [19], who stipulate as a bond condition that the axial stringer strain match the corresponding local sheet strain along the *center-line* of the strip of adhesion – rather than the average sheet strain across the width of this strip. The resulting integro-differential equation for p has the same structure as (3.10); moreover, the new influence function thus emerging, while different from $\hat{\epsilon}$, has precisely the same jump discontinuity. Consequently, the characterization of p may again be reduced to a Fredholm integral equation with the aid of an integration by parts. This reduction is performed explicitly in Section 3 of [4], which includes a corrected[5] and more economical version of the analysis pursued in [19].

Figure 8 shows a comparison of the load-diffusion arrived at on the basis of the two alternative area-contact schemes with experimental results obtained by Goodier and Hsu [14]. The graphs displayed here pertain to a stringer of rectangular cross section with a stiffness-ratio $\kappa=h_sE_s/hE=1$ and a length-ratio $\ell/a=6$. The initial slope of the solid load-diffusion curve is infinite in accordance with the asymptotic estimate (3.15); the logarithmic infinity of $p'(x)$ at $x=\ell$ is not discernible on the scale of Fig. 8. The agreement between the two *theoretical* curves is seen to be quite satisfactory over the entire range of the attachment. In contrast, the comparison between theory and experiment is favorable only sufficiently far from the edge of the sheet. Both theoretical solutions predict that about sixty percent of the applied load is transferred to the sheet abruptly through edge bond-forces at $x_2=0$. The corresponding value furnished by (3.9) is fifty percent, the experimental value being roughly thirty-five percent. On the other hand, all three curves indicate, in surprisingly close mutual agreement, that less than eight percent of the load is transmitted to the sheet at the end of the stringer.

The substantial discrepancies between theory and experiment revealed in Fig. 8 are no doubt due in part to the low stiffness-ratio ($\kappa=1$) underlying the Goodier-Hsu [14] measurements of the axial

[1] See Equation (42) in [4] for an explicit representation of $K(x,\xi)$.

[2] See Section 3 of [4] for details.

[3] See the numerical results discussed at the end of this section.

[4] Observe that $p'(x)\to\infty$ or $p'(x)\to-\infty$ as $x\to\ell$ depending on whether $\nu>1/3$ or $\nu<1/3$, if $p(\ell)>0$.

[5] The work reported in [19] contains an algebraic error pointed out in [4].

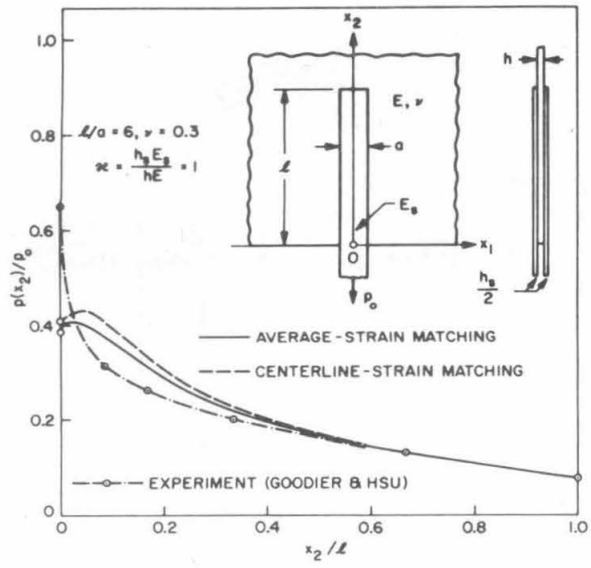

FIG. 8 REISSNER'S PROBLEM. AREA CONTACT. COMPARISON OF THEORY WITH EXPERIMENT

stringer strain.[1] The quality of the two theoretical solutions under discussion is certain to improve with increasing values of κ. On the other hand, it should be kept in mind that the one-dimensional approximations employed in either solution are bound to be least adequate near the junction of the stringer and the edge of the sheet.

4. A PILOT STUDY FOR A CLASS OF THREE-DIMENSIONAL LOAD-TRANSFER PROBLEMS

At this stage we leave the subject of *plane* load transfer and proceed to a discussion of problems involving the transfer of load between an elastic bar and a *three-dimensional* elastic medium (elastic matrix). In this connection we describe first a pilot study contained in [5].[2] The specific problem treated there concerns the diffusion of an axial load from a cylindrical bar B, which is fully immersed in – and continuously bonded to – an infinite matrix M occupying the remainder of the space (Fig. 9). The loading applied to the bar is assumed to be uniformly distributed over one of its cross sections and our primary aim is to determine the decay of the axial bar-force as a measure of the ensuing load-diffusion. While this problem is decidedly artificial, it offers the advantage of lending itself to a solution exact within three-dimensional elastostatics, if the bar is of *circular* cylindrical shape. For this reason, it furnishes a convenient vehicle for testing the quality of an approximative scheme devised in [5], which enables one to cope with a physically interesting class of related spatial load-transfer problems that are no longer readily amenable to a rigorous solution, even for bars of circular cross section.

Although the problem under consideration is evidently a three-dimensional analogue of Melan's first problem, it does not admit an approximate treatment strictly analogous to that employed in Section 1. The nature of this complication is easily explained. Let E, ν and E_b, ν_b be the usual elastic constants of the matrix and the bar, respectively, and call A the cross-sectional area of the bar. Choose rectangular cartesian coordinates (x_1, x_2, x_3) as shown in Fig. 9 and suppose the given load of magnitude p_o is applied in the negative x_3-direction to the cross section Π_o situated at $x_3 = 0$. Next, viewing the bar as a one-dimensional elastic continuum, denote by $p(x)$, $\sigma(x)$, $\epsilon(x)$, and $q(x)$, in this order, the values at $x_3 = x$ of the scalar bar-force, the axial normal stress in B, the corresponding extensional strain, and the scalar bond-force per unit length exerted by M on B. Then (1.2) (with E_s replaced by E_b) and (1.3) clearly apply to the present circumstances, provided f once again stands for the lineal density of a statically equivalent replacement loading obeying (1.1). Moreover, if one were to adhere to the hypothesis of ideal line-contact between the bar and the matrix, one would *formally* be led to the bond condition (1.4), provided $\overset{\circ}{\epsilon}(x)$ now represents the extensional strain parallel to the x_3-axis, at the point $(0, 0, x)$, due to a unit concentrated load acting at the origin in the negative x_3-direction. From Kelvin's solution[3] for an all-around infinite elastic solid under an internal concentrated load one has

$$\overset{\circ}{\epsilon}(x) = \frac{1+\nu}{2\pi E}\,\frac{\operatorname{sgn} x}{x^2} \qquad (0 < |x| < \infty) \tag{4.1}$$

instead of (1.10). Because of the increased order of the singularity at $x = 0$ displayed by $\overset{\circ}{\epsilon}$ in (4.1), as compared to $\overset{\circ}{\epsilon}$ in (1.10), the three-dimensional counterpart of the integral in (1.4) is divergent,[4] so that the spatial analogue of the bond conditon (1.4) is devoid of meaning.

[1] In [4] the theoretically predicted load-diffusion is compared also with photoelastic test results reported in [19], which refer to $K = 2$. Unfortunately, these tests were based on a length-ratio $\ell/a = 3$, for which the present analysis cannot possibly be realistic.

[2] Although this section is, in essence, an abridged version of [5], an attempt is made to improve upon the exposition in [5].

[3] See, for example, Love [20], p. 186.

[4] Thus, in *three* dimensions the strain field induced by a line load fails to be bounded at points of the line of load-application.

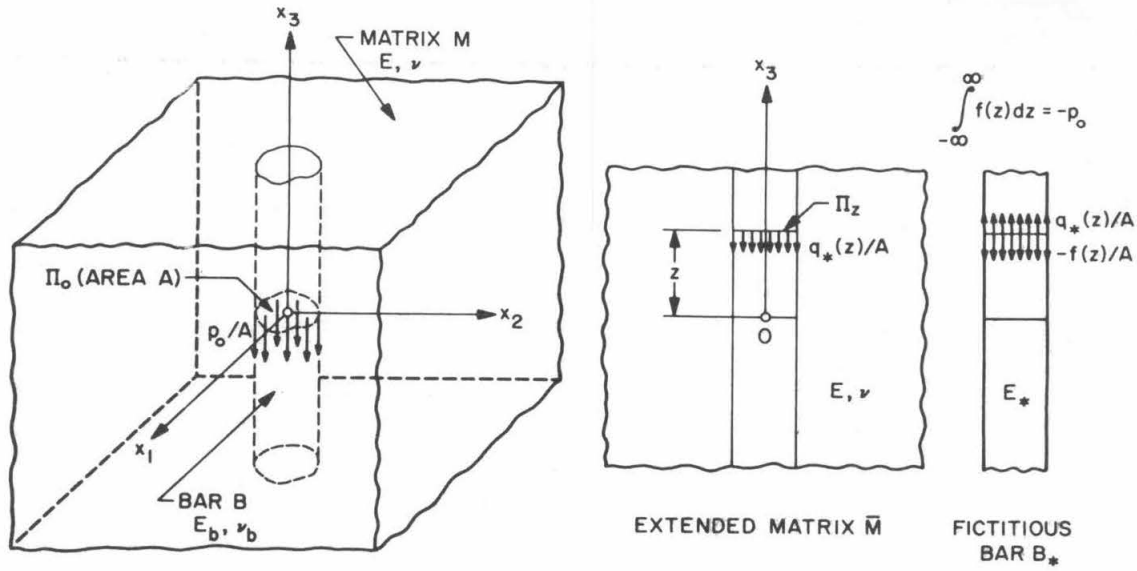

FIG. 9 LOAD-DIFFUSION FROM A BAR INTO AN INFINITE MEDIUM

To circumvent the preceding difficulty, we abandon the line-contact model for the attachment of the bar to the matrix and adopt an approximative scheme suggested by the area-contact treatment of Reissner's problem reviewed in Section 3. As a first step in this direction we extend the original matrix M on to the entire space, stipulating that the extended matrix, hereafter designated by $\bar{M}$, has the elastic constants E and ν appropriate to M. Next, we "superimpose" upon $\bar{M}$, throughout the cylindrical region occupied by the actual bar B, a fictitious reinforcement bar (fictitious stiffener) B_*. This reinforcement is chosen in such a way that the extensional stiffness (Young's modulus) of the artificial "composite solid" occupying the original bar-region is the same as that of B, i.e.,

$$E_* = E_b - E \geq 0 \ , \qquad (4.2)^1$$

where E_* is the modulus of elasticity of B_*. We treat B_* as a one-dimensional elastic continuum and thus assume its behavior governed by the *stress-strain relation*

$$\frac{1}{A} p_*(z) = E_* \epsilon_*(z) \quad (-\infty < z < \infty) \qquad (4.3)$$

together with the *equilibrium equation*

$$p_*'(z) + q_*(z) + f(z) = 0 \quad (-\infty < z < \infty) \ . \qquad (4.4)$$

Here $p_*(z)$ and $\epsilon_*(z)$ are the fictitious scalar bar-force and the axial extensional strain at $x_3 = z$ appropriate to B_*; $q_*(z)$ and $f(z)$ denote, respectively, the fictitious scalar bond-force per unit length exerted by $\bar{M}$ on B_* and the lineal density of the replacement loading, both evaluated at $x_3 = z$.

Let Π_z represent the cross section of the cylindrical bar-region situated at $x_3 = z$. The "bond-forces" exerted by B_* on $\bar{M}$ will be regarded as body forces uniformly distributed over each of the disks Π_z $(-\infty < z < \infty)$ (see Fig. 9); the corresponding scalar resultant force per unit length is evidently given by $-q_*(z)$. Suppose now σ_{ij} and ϵ_{ij} $(i, j = 1, 2, 3)$ denote the cartesian components of the stress and strain fields in the extended matrix due to the preceding body-force distribution. Then,

$$\begin{aligned} \sigma_{ij}(x_1, x_2, x_3) &= \int_{-\infty}^{\infty} q_*(\zeta)\, \hat{\sigma}_{ij}(x_1, x_2, x_3 - \zeta) d\zeta \ , \\ \epsilon_{ij}(x_1, x_2, x_3) &= \int_{-\infty}^{\infty} q_*(\zeta)\, \hat{\epsilon}_{ij}(x_1, x_2, x_3 - \zeta) d\zeta \ , \end{aligned} \qquad (4.5)$$

where $\hat{\sigma}_{ij}$ and $\hat{\epsilon}_{ij}$ are the stresses and strains in the body $\bar{M}$ due to a uniform distribution of body forces over the disk Π_o acting in the negative x_3-direction, the resultant force having unit magnitude. In analogy to the average-strain matching scheme used in Section 3, we impose the *kinematic bond condition*

[1] Poisson's ratio of B_* will not enter into our considerations. Note that the inequality in (4.2) rules out the physically uninteresting case $E_b < E$.

$$\epsilon_*(z)=\frac{1}{A}\int_{\Pi_z}\epsilon_{33}(x_1,x_2,x_3)\,dA\ (-\infty<z<\infty)\,. \qquad (4.6)$$

Finally, we postulate that the actual bar-force $p(z)$ is the sum of the fictitious bar-force $p_*(z)$ and the resultant of the normal tractions on Π_z arising from the stresses in the extended matrix. Accordingly,

$$p(z)=p_*(z)+\int_{\Pi_z}\sigma_{33}(x_1,x_2,x_3)\,dA\ (-\infty<z<\infty)\,. \qquad (4.7)$$

In order to simplify the foregoing system of equations it is expedient to introduce auxiliary influence funtions through

$$\hat{\sigma}(z)=\frac{1}{A}\int_{\Pi_z}\hat{\sigma}_{33}(x_1,x_2,x_3)\,dA\ \ (0<|z|<\infty)\,,\ \hat{\sigma}(0)=\hat{\sigma}(0+)\,,$$

$$\hat{\epsilon}(z)=\frac{1}{A}\int_{\Pi_z}\hat{\epsilon}_{33}(x_1,x_2,x_3)\,dA\ \ (0<|z|<\infty)\,,\ \hat{\epsilon}(0)=\hat{\epsilon}(0+)\,, \qquad (4.8)$$

The physical significance of $\hat{\sigma}(z)$ and $\hat{\epsilon}(z)$ is immediate from (4.8): they are evidently the appropriate stress and strain averages over the cross section Π_z, corresponding to the loading on Π_o underlying the fields $\hat{\sigma}_{ij}$ and $\hat{\epsilon}_{ij}$. Further, for a bar of specified cross-sectional shape, explicit integral representations of $\hat{\sigma}$ and $\hat{\epsilon}$ are obtainable from Kelvin's basic singular solution. Equations (4.6), (4.7), in view of (4.2) to (4.5) and (4.8), after a reversal in the order of the two integrations involved, reduce to

$$\frac{p_*(z)}{A(E_b-E)}+\int_{-\infty}^{\infty}[p_*'(\zeta)+f(\zeta)]\,\hat{\epsilon}(z-\zeta)\,d\zeta=0\ (-\infty<z<\infty), \qquad (4.9)^1$$

$$p(z)=p_*(z)-A\int_{-\infty}^{\infty}[p_*'(\zeta)+f(\zeta)]\,\hat{\sigma}(z-\zeta)\,d\zeta\ (-\infty<z<\infty)\,. \qquad (4.10)$$

Since the integrals in (4.9), (4.10) are both of the convolution type, this pair of equations may be solved for the actual bar-force $p(z)$ by means of the exponential Fourier transform, once the influence functions $\hat{\sigma}$ and $\hat{\epsilon}$ have been determined from Kelvin's solution. In this manner one finds for the special case of a *circular bar* of radius a, on passing to the limit[2] as $\delta\to 0$, that

$$p(z)=\frac{p_o}{2}+\frac{p_o}{\pi}\int_0^{\infty}\frac{E\,\psi(s)}{(1-\nu)E+(1+\nu)(E_b-E)[1-2\nu+\phi(s)]}\times\frac{\sin(zs)}{s}\,ds\ \ (0<z<\infty)\,, \qquad (4.11)^3$$

where

$$\phi(s)=1-2K_1(as)\,[asI_o(as)-2\nu I_1(as)]\ \ (0<s<\infty)\,,$$

$$\psi(s)=1-2K_1(as)\,[asI_o(as)-\nu I_1(as)]\ \ (0<s<\infty)\,,$$

$$\phi(0)=-(1-2\nu)\,,\ \psi(0)=-(1-\nu)\,, \qquad (4.12)$$

while I_n and K_n are the nth order modified Bessel functions of the first and second kind, respectively. We now cite from [5] the following asymptotic estimates pertaining to $p(z)$, all of which are based on the *approximate solution* (4.11):

$$p(z)=\frac{p_o}{2}+o(1)\ \text{as}\ z\to 0\,,$$

$$p(z)=\frac{p_o(1+\nu)E_b}{2E}\left[1-\frac{\nu(1-2\nu)E}{2(1-\nu^2)E_b}\right]\frac{a^2}{z^2}+o(z^{-2})\ \text{as}\ z\to\infty\,,$$

$$p'(z)=\frac{p_o(1-2\nu)E}{2\pi a[(1-\nu)E+(1+\nu)(1-2\nu)(E_b-E)]}\times\log(z/a)+O(1)\ \text{as}\ z\to 0\,. \qquad (4.13)$$

These estimates are analogous to the asymptotic results for Melan's first problem appearing in (1.9). According to the last of (4.13), the slope of the load-diffusion curve again becomes unbounded as $x\to 0$; indeed, for $0\le\nu<1/2$ and $E_b\ge E$ the coefficient of the logarithm is positive, so that $p'(z)\to-\infty$ as $z\to 0$.

If the cross section of the bar is restricted to be circular, it is not difficult to establish a rigorous three-dimensional solution of the load-diffusion problem at hand. The exact formulation of this problem demands first of all that one satisfy the field

[1] Here we have temporarily ruled out the degenerate case $E_b=E$.

[2] Recall (1.1).

[3] This result is found to hold true also for $E_b=E$.

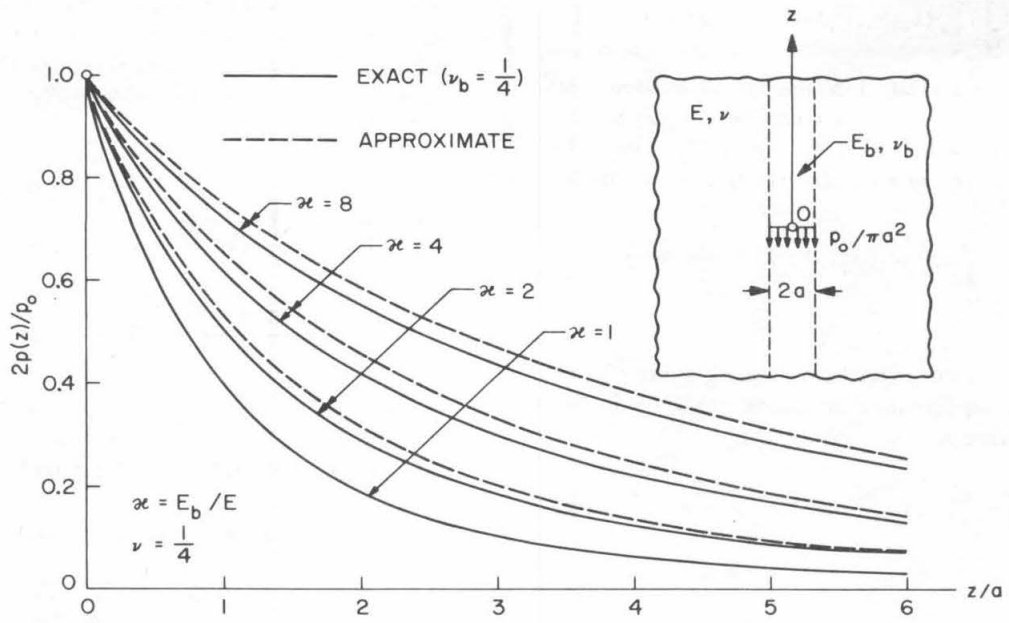

FIG. 10 LOAD-DIFFUSION FROM A BAR INTO AN INFINITE MEDIUM. DECAY OF THE AXIAL BAR-FORCE FOR A CIRCULAR BAR

equations of classical elastostatics throughout the interiors of the matrix and the bar, the latter being subjected to body forces supplied by the previously introduced replacement loading. To these field equations one needs to add the requirement that all stresses vanish at infinity and that the displacements as well as the tractions be continuous at the interface between bar and matrix. The axisymmetric boundary-value problem thus emerging may be attacked efficiently with the aid of Love's stress function and the Fourier transform.[1] This straightforward, if rather laborious, procedure yields a solution in integral form, from which an exact integral representation for the bar-force – analogous to the approximate formula (4.11) – is readily established on letting the assumed (regular) body-force loading tend to the (singular) disk loading depicted in Fig. 9. We record here merely the subsequent asymptotic results furnished by the *exact solution:*

$$p(z)=\frac{p_o}{2}+o(1) \text{ as } z\to 0 ,$$

$$p(z)=\frac{p_o(1+\nu)E_b}{2E}\left[1-\frac{\nu_b(1-2\nu_b)E}{(1+\nu_b)(1-2\nu_b)E+(1+\nu)E_b}\right]\frac{a^2}{z^2}+o(z^{-2})$$

$$\text{as } z\to\infty , \qquad (4.14)$$

$$p'(z)=\frac{p_o}{\pi a}\left[\frac{1}{1+(3-4\nu)\rho}+\frac{1-4\nu_b}{\rho+3-4\nu_b}\right]\log(z/a)+O(1)$$

$$\text{as } z\to 0 ,$$

where

$$\rho=\frac{1+\nu}{1+\nu_b}\kappa , \quad \kappa=\frac{E_b}{E}. \qquad (4.15)^2$$

According to the second of (4.14) and the second of (4.13), $p(z)$ decays as $1/z^2$ in either solution, as $z\to\infty$. Further, if Δ is the ratio of the term dominating the remote behavior of $p(z)$ in (4.14) to its counterpart in (4.13), one easily confirms the bounds

$$\frac{7}{8}\le 1-\frac{1}{\kappa/8}<\Delta<\frac{1}{1-1/14\kappa}\le\frac{14}{13} \qquad (4.16)$$

$$(\kappa\ge 1,\ 0\le\nu\le\tfrac{1}{2},\ 0\le\nu_b\le\tfrac{1}{2}) .$$

[1] See Section 1 of [5] for details.

[2] Thus ρ is the ratio of the shear modulus of the bar to that of the matrix.

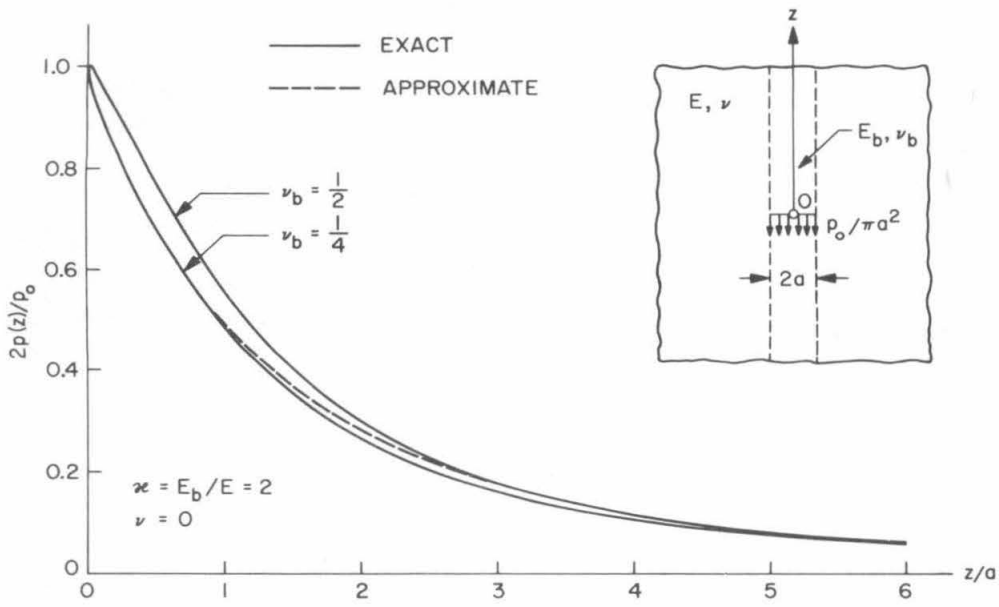

FIG. 11 LOAD-DIFFUSION FROM A BAR INTO AN INFINITE MEDIUM. DECAY OF THE AXIAL BAR-FORCE FOR A CIRCULAR BAR

Consequently, the agreement between the approximate and the exact values of p at large distances from the load is quite favorable – especially for a relatively stiff bar. On the other hand, the estimates (4.13) are identical with (4.14) when $E_b = E$ and $\nu_b = \nu$ since the approximate solution evidently becomes exact if the bar and the surrounding medium have the same elastic properties. Although $p'(z)$ and hence the actual bond-force density $q(z)$ are seen to be logarithmically unbounded at $z = 0$ in both solutions, the last of (4.14) reveals a curious anomaly inherent in the exact solution, i.e.,

$$p'(z) \to +\infty \text{ as } z \to 0 \text{ if } \nu_b > \frac{1}{4} + \frac{2+\rho}{4[2+(3-4\nu)\rho]}, \tag{4.17}$$

in which case the bar-force p is an *increasing* function in an interval adjacent to the loaded cross section. This eventuality is evidently precluded for $\nu_b \leq 1/4$. Finally, it is of interest to compare the asymptotic estimates (4.13), (4.14) with the analogous estimates (1.9), which apply to the approximate solution of Melan's first problem.

Figures 10 and 11 show illustrative quantitative results for the load-diffusion predicted by the exact and by the approximate solution. Figure 10 refers to $\nu = 1/4$ and various values of the stiffness-ratio $\kappa = E_b/E$. The solid curves displayed here are based on the exact solution and correspond to $\nu_b = 1/4$; the dashed curves represent the approximate solution, which is independent of ν_b. For $\kappa = 1$ the solid and the dashed curve coalesce, as must be the case. The initial tangent of all load-diffusion curves is vertical in accordance with the asymptotic results of $p'(z)$ in (4.13) and (4.14). If $\kappa > 1$ the approximate values of $p(z)$ are somewhat larger than the exact values at all $z > 0$. For the choices of κ used in Fig. 10, the maximum discrepancy occurs at $\kappa = 4$, $z \doteq 3a$ and amounts to about ten percent of the exact value of $p(z)$. The rapidity of the load-transfer declines as the stiffness-ratio κ is increased. Even for $\kappa = 8$, however, the bar-force at a distance of three bar-diameters from the loaded cross section is less than fifteen percent of the total applied load p_o. Figure 11, which has not been published previously, relates to the parameter values $\kappa = 2$, $\nu = 0$, and $\nu_b = 1/4$ or $\nu_b = 1/2$. The solid curve corresponding to $\nu_b = 1/2$ exhibits the anomaly predicted by (4.17), but the initial rise in the magnitude of the bar-force is barely noticeable on the scale of this drawing.

The asymptotic and numerical results discussed above supply favorable evidence as to the adequacy of the approximative method described in this section. The remaining sections deal with applications of this method to three-dimensional load-transfer problems of more immediate physical interest.

5. LOAD-TRANSFER TO A HALF-SPACE FROM A PARTIALLY EMBEDDED AXIALLY LOADED ROD

We summarize next a study [6] devoted to a three-dimensional analogue of Reissner's plane load-transfer problem, which was discussed in Section 3. Our present objective is the diffusion of an axial load from a bar of arbitrary uniform cross section that is immersed in, up to a finite depth, and continuously bonded to a semi-infinite solid of distinct elastic properties (Fig. 12). This problem may be attacked by the approximate method applied in the preceding section to a spatial counterpart of Melan's first problem.

Let (x_1, x_2, x_3) be the rectangular cartesian coordinates indicated in Fig. 12 and assume the x_3-axis coincident with the longitudinal centroidal axis of the bar B. We call ℓ the length of the submerged bar segment and denote by Π_o, Π_z $(0<z<\ell)$, and Π_ℓ the cross sections of B located at $x_3=0$, $x_3=z$, $x_3=\ell$, respectively. Otherwise we adhere to the notation employed in Section 4. The immersed portion of B occupies a cylindrical subregion of the half-space $x_3\geq 0$, the remainder of which is taken up by the matrix M. The entire loading is supposed to be confined to the projecting portion of the bar and is presumed statically equivalent to a force of magnitude p_o acting in the negative x_3-direction and having the x_3-axis as its line of action.

The "extended matrix" $\bar{M}$, in the present circumstances, occupies the complete half-space $x_3\geq 0$ and its "fictitious reinforcement" B_* (over the region occupied by the immersed part of B) obeys the one-dimensional characterization

$$\frac{1}{A}\,p_*(z)=E_*\epsilon_*(z)\ ,\ p_*'(z)+q_*(z)=0\ \ (0<z<\ell)\,. \tag{5.1}$$

Here E_* again satisfies (4.2), while A, $p_*(z)$, $\epsilon_*(z)$, and $q_*(z)$ have the same meaning as in (4.3), (4.4).

The forces external with respect to $\bar{M}$ consist of distributed bond-forces of scalar lineal density $-q_*(z)$ $(0<z<\ell)$, together with the load-portion $p_o-p_*(0)$ transmitted to $\bar{M}$ directly at $x_3=0$ and the bond-force of magnitude $p_*(\ell)$ communicated to $\bar{M}$ abruptly at $x_3=\ell$. All of these fictitious bond-forces are regarded as body forces acting on the semi-infinite solid $\bar{M}$ and are assumed to be uniformly distributed over the respective plane regions Π_z $(0<z<\ell)$, Π_o, and Π_ℓ (see Fig. 12). The stresses and strains induced in $\bar{M}$ by the foregoing force system evidently admit the representation

$$\sigma_{ij}(\mathbf{x})=[p_o-p_*(0)]\,\hat{\sigma}_{ij}(\mathbf{x},\,0)+p_*(\ell)\hat{\sigma}_{ij}(\mathbf{x},\ell)+\int_0^\ell q_*(\zeta)\,\hat{\sigma}_{ij}(\mathbf{x},\zeta)\,d\zeta\,, \tag{5.2}$$

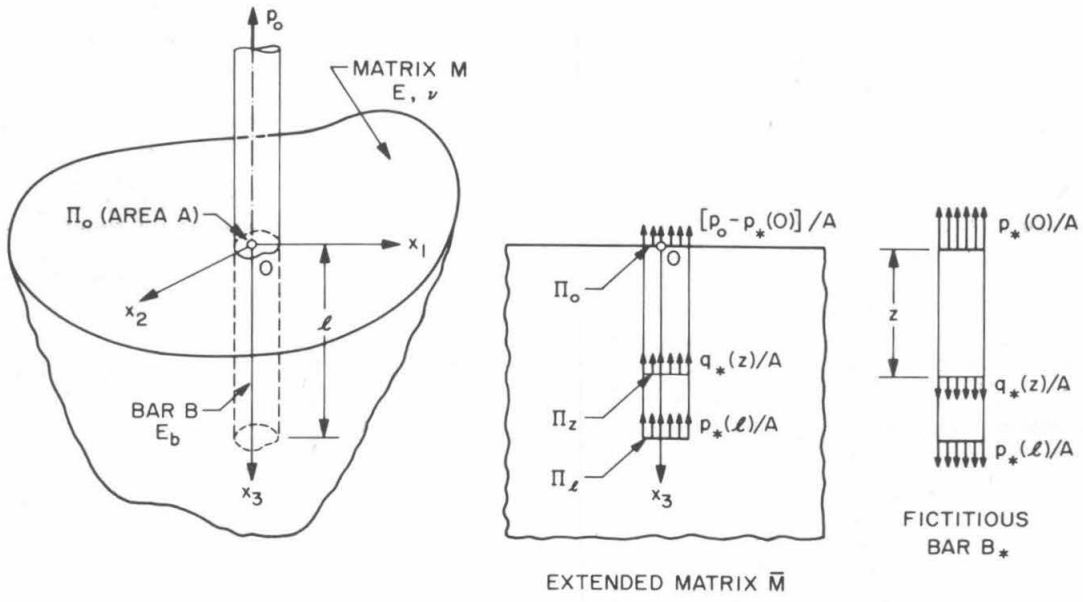

FIG. 12 LOAD-DIFFUSION FROM A BAR INTO A HALF-SPACE

$$\epsilon_{ij}(\mathbf{x}) = [p_o - p_*(0)]\,\hat{\epsilon}_{ij}(\mathbf{x}, 0) + p_*(\ell)\,\hat{\epsilon}_{ij}(\mathbf{x}, \ell) + \int_0^\ell q_*(\zeta)\,\hat{\epsilon}_{ij}(\mathbf{x}, \zeta)\,d\zeta\,,$$

provided $\mathbf{x} = (x_1, x_2, x_3)$, whereas $\hat{\sigma}_{ij}(\mathbf{x}, \zeta)$ and $\hat{\epsilon}_{ij}(\mathbf{x}, \zeta)$ are the stresses and strains at $\mathbf{x}$ due to a uniform body-force distribution over the disk Π_ζ, acting in the negative x_3-direction, the resultant applied force having unit magnitude. In place of (4.6) one now has the bond condition

$$\epsilon_*(z) = \frac{1}{A}\int_{\Pi_z} \epsilon_{33}(x_1, x_2, x_3)\,dA \quad (0 \le z \le \ell)\,, \tag{5.3}$$

and (4.7) here gives way to

$$p(z) = p_*(z) + \int_{\Pi_z} \sigma_{33}(x_1, x_2, x_3)\,dA \quad (0 \le z \le \ell)\,. \tag{5.4}$$

Next, in analogy to (4.8), we define a pair of auxiliary influence functions through

$$\hat{\sigma}(z, \zeta) = \frac{1}{A}\int_{\Pi_z} \hat{\sigma}_{33}(\mathbf{x}, \zeta)\,dA \quad (0 \le z \le \ell,\ 0 \le \zeta \le \ell,\ z \ne \zeta)\,,$$
$$\hat{\epsilon}(z, \zeta) = \frac{1}{A}\int_{\Pi_z} \hat{\epsilon}_{33}(\mathbf{x}, \zeta)\,dA \quad (0 \le z \le \ell,\ 0 \le \zeta \le \ell,\ z \ne \zeta) \tag{5.5}$$

with the supplementary requirements that

$$\hat{\sigma}(0,0) = \hat{\sigma}(0+,0)\,,\quad \hat{\sigma}(\ell,\ell) = \hat{\sigma}(\ell-,\ell)\,,$$
$$\hat{\epsilon}(0,0) = \hat{\epsilon}(0+,0)\,,\quad \hat{\epsilon}(\ell,\ell) = \hat{\epsilon}(\ell-,\ell)\,. \tag{5.6}$$

The physical significance of $\hat{\sigma}(z, \zeta)$ and $\hat{\epsilon}(z, \zeta)$ is easily accounted for: they evidently represent the averages over Π_z of the normal stress on Π_z and of the extensional strain parallel to the x_3-axis induced in the semi-infinite solid $\overline{M}$ by the disk loading on Π_ζ underlying the influence fields $\hat{\sigma}_{ij}(\mathbf{x}, \zeta)$ and $\hat{\epsilon}_{ij}(\mathbf{x}, \zeta)$ introduced earlier in connection with (5.2). Integral representations of the functions $\hat{\sigma}$ and $\hat{\epsilon}$ are readily established with the aid of Mindlin's [21, 22] basic singular solution for a half-space under an internal concentrated load.

On combining (5.1), (5.2), (5.3), (5.4), (4.2) with (5.5), one arrives at

$$\frac{p_*(z)}{A(E_b - E)} - [p_o - p_*(0)]\,\hat{\epsilon}(z, 0) - p_*(\ell)\,\hat{\epsilon}(z, \ell) + \int_0^\ell p_*'(\zeta)\,\hat{\epsilon}(z, \zeta)\,d\zeta = 0 \quad (0 < z < \ell)\,, \tag{5.7}$$

[1]

$$p(z) = p_*(z) + A\left\{[p_o - p_*(0)]\,\hat{\sigma}(z, 0) + p_*(\ell)\,\hat{\sigma}(z, \ell) - \int_0^\ell p_*'(\zeta)\,\hat{\sigma}(z, \zeta)\,d\zeta\right\} \quad (0 < z < \ell)\,. \tag{5.8}$$

Equations (5.7), (5.8) are essentially more complicated than (4.9), (4.10) since the kernels $\hat{\epsilon}$ and $\hat{\sigma}$ in (5.7), (5.8) are not of the translation type and because of the finite range of integration. While it is not feasible to solve (5.7), (5.8) explicitly by analytical means, it is possible to transform the integro-differential equation (5.7) into an ordinary integral equation and, at the same time, to cast (5.8) into a more convenient form by a procedure which is parallel to that used previously in reducing (3.10) to (3.13). As a prerequisite for this task we state first certain conclusions concerning the structure of the influence functions $\hat{\epsilon}$ and $\hat{\sigma}$ defined in (5.5). As was proved in [6] with the aid of Mindlin's solution and potential-theoretic considerations,

$$\hat{\epsilon}(z, \zeta) = \frac{(1+\nu)(1-2\nu)}{2(1-\nu)EA}\,\mathrm{sgn}(z-\zeta) + R_1(z, \zeta)\,,$$
$$\hat{\sigma}(z, \zeta) = \frac{1}{2A}\,\mathrm{sgn}(z-\zeta) + R_2(z, \zeta) \tag{5.9}$$
$$(0 \le z \le \ell,\ 0 \le \zeta \le \ell,\ z \ne \zeta)\,,$$

where $R_1(z, \zeta)$, $R_2(z, \zeta)$ are functions "regular" in the sense of being continuous for $0 \le z \le \ell$, $0 \le \zeta \le \ell$ and continuously differentiable for $0 \le z \le \ell$, $0 \le \zeta \le \ell$ $(z \ne \zeta)$. Accordingly, $\hat{\epsilon}$ and $\hat{\sigma}$ exhibit merely finite jump discontinuities, which are characterized by

$$\hat{\epsilon}(z, z-) - \hat{\epsilon}(z, z+) = \frac{(1+\nu)(1-2\nu)}{(1-\nu)AE}\,,\quad \hat{\sigma}(z, z-) - \hat{\sigma}(z, z+) = \frac{1}{A}\,. \tag{5.10}$$

Bearing (5.10) in mind and applying an integration by parts to the integrals in (5.7), (5.8), one is led to

[1] The degenerate case in which $E_b = E$ requires separate attention. See (5.15).

$$\frac{1}{A}\left[\frac{1}{E_b - E} + \frac{(1+\nu)(1-2\nu)}{(1-\nu)E}\right] p_*(z) - \int_0^\ell p_*(\zeta) K_1(z,\zeta)\, d\zeta \tag{5.11}$$

$$= p_o\, \hat{\epsilon}(z,0) \quad (0 \le z \le \ell),$$

$$p(z) = p_o\, A\, \hat{\sigma}(z,0) + A \int_0^\ell p_*(\zeta) K_2(z,\zeta)\, d\zeta \quad (0 \le z \le \ell), \tag{5.12}$$

provided

$$K_1(z,\zeta) = \frac{\partial}{\partial \zeta}\, \hat{\epsilon}(z,\zeta), \quad K_2(z,\zeta) = \frac{\partial}{\partial \zeta}\, \hat{\sigma}(z,\zeta) \tag{5.13}$$

$$(0 \le z \le \ell,\ 0 \le \zeta \le \ell,\ z \ne \zeta).$$

These kernels are integrable because of (5.9) and the regularity properties of R_1, R_2 described before.

For a given cross section of the bar one may establish[1] explicit representations, in integral form, for the influence functions $\hat{\epsilon}$, $\hat{\sigma}$ and the kernels K_1, K_2 by recourse to the definition of the former and by invoking (5.9), (5.13), as well as the solution to Mindlin's problem [21, 22]. Accordingly, (5.11) constitutes an integral equation of Fredholm's second kind for the fictitious bar-force $p_*(z)$ $(0 \le z \le \ell)$, which lends itself to a numerical solution. Once p_* has been found, the desired actual bar-force $p(z)$ $(0 \le z \le \ell)$ may be computed from (5.12). The latter equation is found to imply

$$p(0) = p_o, \tag{5.14}$$

so that – in contrast to the predictions arising from the area-contact treatment of Reissner's problem (see Fig. 8) – there is no concentrated load-transfer at the initial cross section of the attached bar segment. Since (5.7) is invalid when $E_b = E$, the same is true of (5.11). It is easily confirmed that for $E_b = E$,

$$p_*(z) = 0 \ (0 \le z \le \ell), \quad p(z) = p_o A \hat{\sigma}(z,0) \ (0 < z \le \ell),$$

$$p(0) = p_o. \tag{5.15}$$

We turn now to the special case of a bar of *circular cross section*. As demonstrated in Section 2 of [6], the functions $\hat{\epsilon}$, $\hat{\sigma}$ and K_1, K_2 are in this instance expressible in terms of elementary functions and complete elliptic integrals of the first and second kind. Also, if a denotes the radius of the bar, one has at present[2]

$$K_1(z,\zeta) = -\frac{1+\nu}{2\pi^2 a^3 (1-\nu) E}\left[(1-4\nu)\log\frac{|z-\zeta|}{a}\right.$$

$$\left. -(1-4\nu+8\nu^2)\log\frac{z+\zeta}{a}\right] + M_1(z,\zeta), \tag{5.16}$$

$$K_2(z,\zeta) = -\frac{1-2\nu}{2\pi^2 a^3 (1-\nu)}\log\frac{|z-\zeta|}{z+\zeta} + M_2(z,\zeta),$$

where $M_1(z,\zeta)$ and $M_2(z,\zeta)$ are functions continuous for $0 < z \le \ell$, $0 < \zeta \le \ell$, which possess finite limits as the origin of the (z,ζ)-plane is approached along a fixed direction. Next, we append the asymptotic estimates (deduced in [6]):

$$p'(z) = O(1) \text{ as } z \to 0,$$

$$p'(z) = \frac{(1-2\nu)\, p_*(\ell)}{2\pi(1-\nu)a}\log[(\ell - z)/\ell] + O(1) \text{ as } z \to \ell. \tag{5.17}$$

Thus p', and hence the *actual* bond-force density q, remain finite at the boundary of the matrix. On the other hand, p' and q become logarithmically infinite at the embedded end of the bar.[3]

From among the extensive numerical results appropriate to a circular bar presented in [6] we reproduce here, for illustrative purposes, merely those collected in Fig. 13. The load-diffusion curves appearing in this figure refer to $\nu = 1/4$, to two distinct length-ratios ℓ/a, and to several values of the stiffness-ratio $\kappa = E_b/E$. All curves shown have a finite initial slope, in agreement with the first of (5.17), and represent steadily decreasing functions. The logarithmic infinity of the end-slope at $z = \ell$ does not become conspicuous on the scale of Fig. 13. While there is no concentrated load-transfer at $z = 0$, as predicted by (5.14), a part of the applied load is transferred to the matrix at the terminal cross section of the embedded rod. This load-portion diminishes as ℓ/a is increased and rises with increasing values of κ; it amounts to less than eight percent of the load when $\ell/a = 10$ and $\kappa = 8$.

The load-diffusion is again seen to be less rapid at higher stiffness-ratios. Even for a relatively stiff bar, however, most of the load-transfer occurs in the vicinity of the surface of the matrix and there is quite insensitive to changes of the length-ratio.

[1] See Section 2 of [6].

[2] See Equations (2.19) in [6].

[3] The numerical solution of (5.11) furnishes $p_*(\ell) \ne 0$.

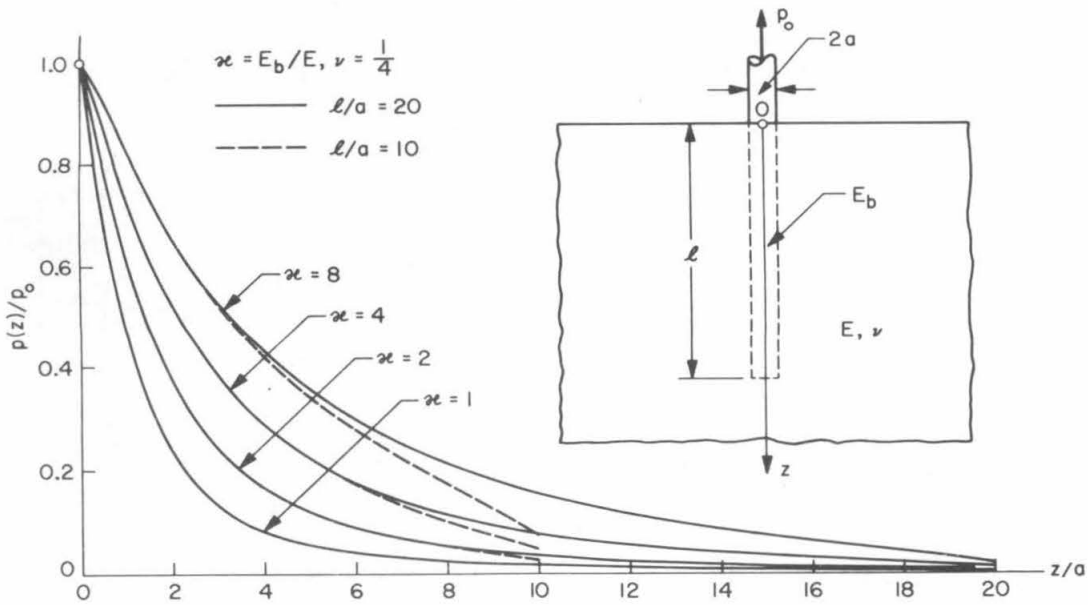

FIG. 13 LOAD-DIFFUSION FROM A BAR INTO A HALF-SPACE. DECAY OF THE AXIAL BAR-FORCE FOR A CIRCULAR BAR

Thus, for $E_b/E \leq 8$ and $\ell = 20a$, over half of the load is transmitted to the matrix by a bar segment in the range $0 \leq z \leq 4a$. Further, in this range the dashed curves, which are based on $\ell/a = 10$, are practically indistinguishable from the corresponding solid curves, which pertain to $\ell/a = 20$. Accordingly, a doubling of the length of the embedded bar portion, from $\ell = 10a$ to $\ell = 20a$, results in little benefit. This finding, though deduced on the assumption of perfectly elastic behavior of the bar and the matrix alike, is apt to be significant for design purposes. Finally, it may be well to emphasize that the analysis reported here is bound to be unrealistic unless the embedded bar-length is sufficiently large compared to the diameter of the bar.

6. *LOAD-ABSORPTION BY A FILAMENT IN A FIBER-REINFORCED COMPOSITE*

Despite numerous recent experimental and theoretical investigations of fiber-reinforced composites, a basic understanding of the mechanics of such materials appears to have lagged behind their successful technological application. The study contained in [7], which is to be reviewed presently, concerns a rather fundamental, if highly idealized, problem in the analysis of fiber-reinforced materials. Leaving aside questions posed by the interaction between individual filaments and barring all failure considerations, we limit our attention to a single elastic fiber that is immersed in, and bonded to, an all-around infinite elastic matrix (see Fig. 14). Further, we assume the fiber to be of uniform circular cross section and, in view of the extreme slenderness of filaments commonly used in actual composites, deal directly with a fiber of semi-infinite extent. The matrix is supposed to be subjected to a homogeneous uniaxial state of stress at infinity, parallel to the axis of the embedded filament. We seek to establish the longitudinal distribution of the fiber-force, which at the same time controls the variation of the bond-tractions at the interface between the fiber and the surrounding medium.

The counterpart of this problem for a filament of finite length and its generalization to multifiber reinforcements, have been the object of analytical work previous to [7]. Thus the literature on the single-fiber problem includes several efforts to arrive at elementary formulas for the interfacial bond-force based on a one-dimensional treatment of both the fiber and the matrix. In contrast, Cohen and Romualdi [23] (1967), aiming at the multifiber problem, propose a numerical solution scheme which rests on a three-dimensional continuum model for the matrix but involves a somewhat rudimentary discretized bond condition.

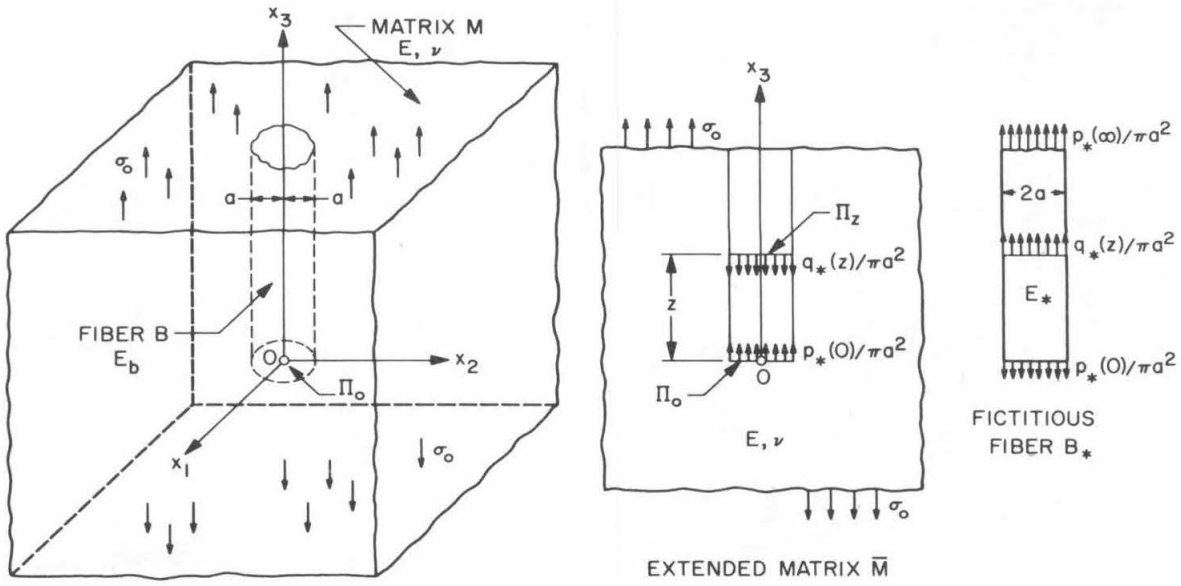

FIG. 14 LOAD-ABSORPTION BY A FILAMENT IN A FIBER-REINFORCED COMPOSITE

The investigation reported in [7] had as its purpose a more refined treatment of the single-fiber problem described above. This objective is accomplished in [7] by yet another application of the approximate scheme developed in [5] and summarized in Section 4. Indeed, the present problem bears a close analytical relationship to the problems discussed in Sections 4 and 5. We may therefore set down its formulation with a minimum of explanatory comment. To this end we introduce the coordinate frame displayed in Fig. 14 and retain the notation originally adopted in Section 4.

The equations stemming from the one-dimensional considerations appropriate to the fictitious reinforcement B_* (fictitious filament) are given by

$$\frac{1}{\pi a^2}\, p_*(z) = E_* \epsilon_*(z)\ ,\ p_*'(z) + q_*(z) = 0\ \ (0 < z < \infty) \tag{6.1}$$

in conjunction with (4.2). On the other hand, the stresses and strains in the extended matrix $\bar{M}$, which occupies the entire space, obey

$$\sigma_{ij}(x_1, x_2, x_3) = \overset{\infty}{\sigma}_{ij} - p_*(0)\, \hat{\sigma}_{ij}(x_1, x_2, x_3) + \int_0^\infty q_*(\zeta)\, \hat{\sigma}_{ij}(x_1, x_2, x_3 - \zeta)\, d\zeta\ , \tag{6.2}$$

$$\epsilon_{ij}(x_1, x_2, x_3) = \overset{\infty}{\epsilon}_{ij} - p_*(0)\, \hat{\epsilon}_{ij}(x_1, x_2, x_3) + \int_0^\infty q_*(\zeta)\, \hat{\epsilon}_{ij}(x_1, x_2, x_3 - \zeta)\, d\zeta\ .$$

Here $\overset{\infty}{\sigma}_{ij}$ and $\overset{\infty}{\epsilon}_{ij}$ denote the stress and strain contributions due to the uniaxial loading at infinity, so that

$$\overset{\infty}{\sigma}_{ij} = \delta_{3i}\delta_{3j}\sigma_o\ ,\ \overset{\infty}{\epsilon}_{ij} = \frac{\sigma_o}{E}\left[(1+\nu)\delta_{3i}\delta_{3j} - \nu\delta_{ij}\right]\ , \tag{6.3}$$

where σ_o is the intensity of the stress applied to the matrix M and δ_{ij}, as before, stands for the Kronecker-delta; the influence fields $\hat{\sigma}_{ij}$ and $\hat{\epsilon}_{ij}$, in turn, are precisely the same as those underlying (4.5). The second term in the right-hand members of (6.2) evidently represents the stresses and strains produced in the extended matrix by the bond-force transmitted to $\bar{M}$ abruptly at the terminal cross section Π_o of B_*. Finally, (6.1), (6.2) are to be accompanied by the bond condition

$$\epsilon_*(z) = \frac{1}{\pi a^2} \int_{\Pi_z} \epsilon_{33}(x_1, x_2, x_3)\, dA\ \ (0 \le z < \infty) \tag{6.4}$$

together with

$$p(z)=p_*(z)+\int_{\Pi_z}\sigma_{33}(x_1,x_2,x_3)\,dA\quad(0\le z<\infty)\,,\tag{6.5}$$

Let $\hat{\sigma}$ and $\hat{\epsilon}$ be the auxiliary influence functions defined in (4.8). These equations and (6.1), (6.2), (6.3) permit one to write (6.4), (6.5) in the form

$$\frac{p_*(z)}{\pi a^2(E_b-E)}=\frac{\sigma_o}{E}-p_*(0)\hat{\epsilon}(z)-\int_0^\infty p_*'(\zeta)\hat{\epsilon}(z-\zeta)d\zeta\quad(0\le z<\infty)\,.\tag{6.6}$$

$$p(z)=p_*(z)+\pi a^2\left[\sigma_o-p_*(0)\,\hat{\sigma}(z)\right.$$
$$\left.\int_0^\infty p_*'(\zeta)\,\hat{\sigma}(z-\zeta)d\zeta\right]\quad(0\le z<\infty)\,.\tag{6.7}$$

In deducing (6.6) we have evidently excluded the degenerate case in which the matrix and the fiber have the same modulus of elasticity. If $E_b=E$, (6.1), (4.2), (6.7) furnish directly

$$p_*(z)=0\,,\ p(z)=\pi a^2\sigma_o\quad(0\le z<\infty)\,.\tag{6.8}$$

Further, for $E_b\ge E$, (6.1), (6.3), (6.4), (6.5) imply

$$p_*(\infty)\equiv\lim_{z\to\infty}p_*(z)=\pi a^2\sigma_o\frac{E_b-E}{E},$$
$$p(\infty)\equiv\lim_{z\to\infty}p(z)=\pi a^2\sigma_o\frac{E_b}{E}\,.\tag{6.9}$$

Clearly, $p(\infty)$ is the reactive actual filament-force induced at infinity by the bond between fiber and matrix.

We now eliminate the derivative of p_* from (6.6), (6.7) by the same procedure that led from (5.7), (5.8) to (5.11), (5.12). For this purpose we note first that the influence functions $\hat{\epsilon}$ and $\hat{\sigma}$ entering (6.6), (6.7), by virtue of their definition, may be represented in integral form with the aid of Kelvin's classical solution for an infinite elastic solid under an internal concentrated load. In this manner one confirms, in analogy to (5.9), that

$$\hat{\epsilon}(z)=\frac{(1+\nu)(1-2\nu)}{2(1-\nu)\pi a^2E}\,\mathrm{sgn}(z)+R_1(z)\,,$$
$$\hat{\sigma}(z)=\frac{1}{2\pi a^2}\,\mathrm{sgn}(z)+R_2(z)\quad(0<|z|<\infty)\,,\tag{6.10}$$

where R_1, R_2 are functions continuous on the entire real axis and continuously differentiable on the open intervals $(-\infty, 0)$, $(0, \infty)$. From (6.10) follows

$$\hat{\epsilon}(0+)-\hat{\epsilon}(0-)=\frac{(1+\nu)(1-2\nu)}{(1-\nu)\pi a^2E},\quad\hat{\sigma}(0+)-\hat{\sigma}(0-)=\frac{1}{\pi a^2}\,.\tag{6.11}$$

Further,

$$\hat{\epsilon}(z)=o(1)\,,\ \hat{\sigma}(z)=o(1)\ \text{as}\ |z|\to\infty\,.\tag{6.12}$$

Equations (6.6), (6.7), upon an integration by parts coupled with an appeal to (6.11), (6.12), and (6.9), pass over into

$$\frac{1}{\pi a^2}\left[\frac{1}{E_b-E}+\frac{(1+\nu)(1-2\nu)}{(1-\nu)E}\right]p_*\,z$$
$$+\int_0^\infty p_*(\zeta)K_1(z-\zeta)\,d\zeta=\frac{\sigma_o}{E}\quad(0\le z<\infty)\,,\tag{6.13}$$

$$p(z)=\pi a^2\sigma_o-\pi a^2\int_0^\infty p_*(\zeta)K_2(z-\zeta)\,d\zeta\quad(0\le z<\infty)\,,\tag{6.14}$$

where

$$K_1(z)=\hat{\epsilon}'(z),\quad K_2(z)=\hat{\sigma}'(z)\quad(0<|z|<\infty)\,.\tag{6.15}$$

The integral equation (6.13), which governs the fictitious filament-force p_*, is one of Fredholm's second kind and (6.14) supplies a direct integral representation, in terms of p_*, for the actual filament-force p. Both R_1, R_2 and K_1, K_2 are expressible in terms of complete elliptic integrals of the first and second kind[1] and the structure of the translation-kernels K_1, K_2 is found to be characterized by

$$K_1(z)=\frac{(1+\nu)(1-4\nu)}{2\pi^2a^3(1-\nu)E}\log\frac{|z|}{a}+M_1(z)\,,$$
$$K_2(z)=\frac{1-2\nu}{2\pi^2a^3(1-\nu)}\log\frac{|z|}{a}+M_2(z)\,,\tag{6.16}$$

[1] See Section 2 of [7].

in which M_1 and M_2 are functions continuous on the entire real axis. Further,

$$K_1(z) = -\frac{1+\nu}{\pi E\,|z|^3} + O(z^{-5}) \text{ as } |z| \to \infty ,$$

$$K_2(z) = -\frac{2-\nu}{2\pi(1-\nu)\,|z|^3} + O(z^{-5}) \text{ as } |z| \to \infty . \tag{6.17}$$

In view of the first of (6.9), it is expedient to change the dependent variable in (6.13) from p_* to the (dimensionless) "complementary fictitious filament-force"

$$\psi(\xi) = 1 - \frac{p_*(z)}{p_*(\infty)} = 1 - \frac{E}{\pi a^2 \sigma_o (E_b - E)}\, p_*(\lambda a \xi) , \tag{6.18}$$

where ξ and λ are the nondimensional variables defined by

$$\xi = \frac{z}{\lambda a}, \quad \lambda = \sqrt{\frac{(1+\nu)(E_b - E)}{2E}} . \tag{6.19}$$

This change of variables eventually carries (6.13) into the Fredholm equation

$$\omega\,\psi(\xi) - \lambda \int_0^\infty \psi(\eta)\, G(\xi - \eta)\, d\eta = \alpha(\xi) \quad (0 \le \xi < \infty) , \tag{6.20}$$

provided,

$$\omega = 2(1-2\nu) = +\frac{1-\nu}{\lambda^2} , \quad G(\xi) = -\frac{2\pi a^3 (1-\nu) E}{1+\nu} K_1(\lambda a \xi) ,$$

$$\alpha(\xi) = \frac{2\pi a^2 (1-\nu) E}{1+\nu}\, \hat{\epsilon}(\lambda a \xi) . \tag{6.21}$$

Moreover, from (6.21), the first of (6.17), (6.19), and the elliptic-integral representation of $\hat{\epsilon}$ follows

$$G(\xi) = \frac{2(1-\nu)}{\lambda^3 |\xi|^3} + O(\xi^{-5}) \text{ as } |\xi| \to \infty ,$$

$$\alpha(\xi) = \frac{1-\nu}{\lambda^2 \xi^2} + O(\xi^{-4}) \text{ as } \xi \to \infty . \tag{6.22}$$

[1] See Section 4 of [7].

As is apparent from (6.18), (6.19), and (6.22), the integral equation (6.20) has the advantage over (6.13) that its unknown function $\psi(\xi)$, as well as its right-hand member $\alpha(\xi)$ tends to zero as $\xi \to \infty$. A precise estimate for $\psi(\xi)$ as $\xi \to \infty$ may be extracted from (6.20) with the aid of (6.22) and a theorem [24] on asymptotic properties of solutions to a class of Fredholm equations that contains (6.20). One thus arrives at

$$\psi(\xi) = \frac{1}{\xi^2} + o(\xi^{-2}) \text{ as } \xi \to \infty . \tag{6.23}$$

It is now clear that the artificial length-scale introduced in (6.19) serves to normalize the far-field behavior of ψ. Equations (6.23), (6.18), (6.19), in conjunction with (6.14), (6.17) and results established in [24], enable one to deduce the estimate

$$\frac{p(z)}{p(\infty)} = 1 - \frac{(1+\nu)(E_b - E)}{2E} \left[1 - \frac{\nu(1-2\nu)E}{2(1-\nu^2)E_b} \right] \left(\frac{a}{z} \right)^2 + o(z^{-2}) \text{ as } z \to \infty \tag{6.24}$$

for the remote behavior of the actual filament-force. Finally, we cite from [7] also the asymptotic formula

$$p'(z) = -q(z) = -\frac{(1-2\nu)\, p_*(0)}{2\pi(1-\nu)\, a} \log \frac{z}{a} + O(1) \text{ as } z \to 0 \tag{6.25}$$

which reveals the nature of the singularity in the *actual* bond-force density $q(z)$ at the end of the fiber.

Equation (6.20) is of the type encompassed by the Wiener-Hopf technique. Because of the unwieldiness of the kernel G, however, it is more efficient to solve (6.20) by direct numerical means. Once $\psi(\xi)$, and thus $p_*(z)$, has been found, the desired actual filament-force $p(z)$ may be determined by evaluating the integral in (6.14) numerically. These calculations can be expedited appreciably if the estimates (6.23) and (6.24) are properly exploited.[1]

We proceed now to a discussion of illustrative numerical results. Figure 15 shows the normalized filament-force $p(z)/p(\infty)$ as a function of position along the axis of the fiber for $\nu = 1/4$ and several choices of the stiffness-ratio $\kappa = E_b/E$. The straight line appropriate to $\kappa = 1$ corresponds to the degenerate case covered by (6.8). The asymptotic results for $\kappa = 2$ and $\kappa = 5$ are based upon (6.24). The curves

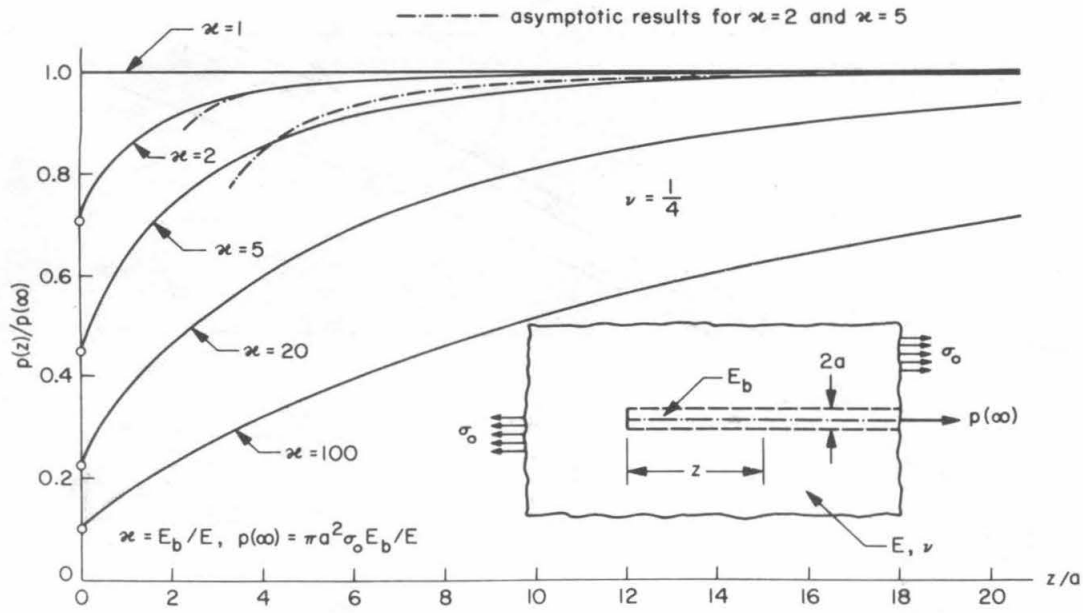

FIG. 15 LOAD-ABSORPTION BY A FILAMENT IN A FIBER-REINFORCED COMPOSITE. VARIATION OF THE AXIAL FILAMENT-FORCE

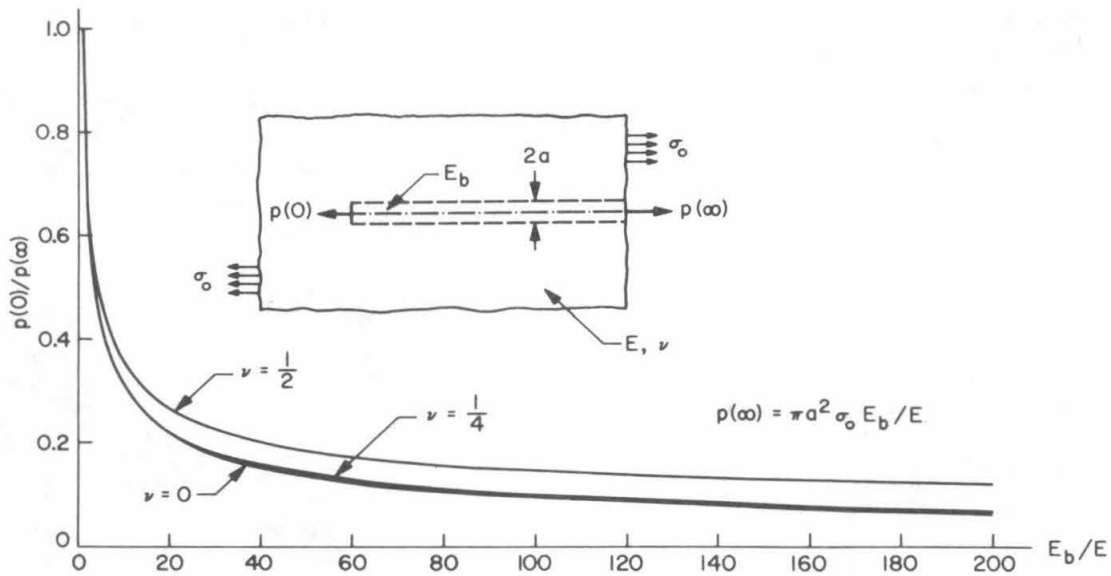

FIG. 16 LOAD-ABSORPTION BY A FILAMENT IN A FIBER-REINFORCED COMPOSITE. DEPENDENCE OF FILAMENT END-FORCE ON STIFFNESS-RATIO

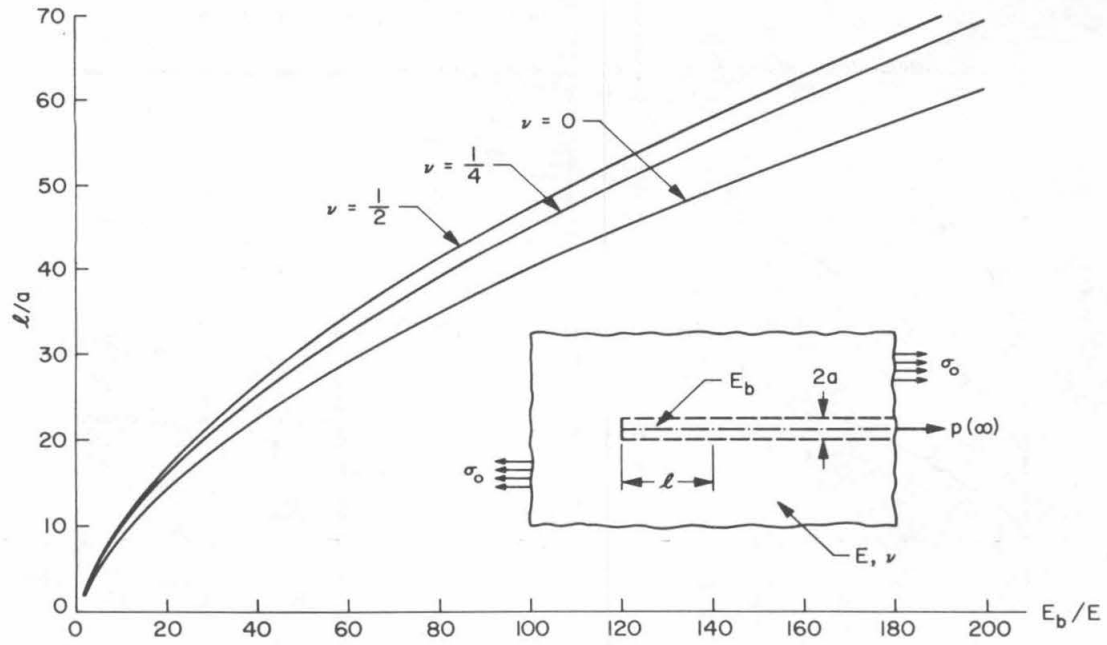

FIG. 17 LOAD-ABSORPTION BY A FILAMENT IN A FIBER-REINFORCED COMPOSITE. DEPENDENCE OF ℓ/a ON STIFFNESS-RATIO FOR $p(\ell)/p(\infty) = 0.9$

in Fig. 15 for which $\kappa > 1$ represent steadily increasing functions and exhibit an infinite initial slope. This unboundedness of the bond-force density at $z=0$ is consistent with (6.25) and reflects a tendency toward debonding in the vicinity of the end of the filament.

As is clear from Fig. 15, the solution under discussion predicts that a portion of the total load $p(\infty)$ absorbed by the filament is transferred to the latter directly at its end $z=0$. This load-portion diminishes as the relative fiber-stiffness increases. Figure 16 depicts the dependence of $p(0)/p(\infty)$ upon $\kappa = E_b/E$ for three values of the Poisson-ratio ν. It is interesting to note that while $p(0)/p(\infty)$ declines rapidly with growing κ near $\kappa=1$, $p(0)$ is still approximately ten percent of $p(\infty)$ for $\kappa=100$ if $\nu = 1/4$.

While the full fiber-load $p(\infty)$ is proportional to E_b/E, the *rate* at which this limiting value is approached decreases with rising values of the stiffness-ratio. In this sense the prevailing load-transfer is less efficient for a comparatively stiff filament. In order to arrive at a quantitative index for the effectiveness of the load-absorption we call ℓ the distance from the end of the filament at which the fiber-force attains ninety percent of $p(\infty)$.

Figure 17 displays ℓ/a as a function of E_b/E for $\nu=0$, $\nu=1/4$, and $\nu=1/2$. Once $E_b/E > 100$ this relationship is seen to become linear for all practical purposes.

ACKNOWLEDGMENT

The author is greatly indebted to Rokuro Muki, who read the manuscript and offered numerous most valuable criticisms and suggestions.

REFERENCES

[1] E. Melan, "Ein Beitrag zur Theorie geschweisster Verbindungen," *Ingenieur Archiv*, vol. 3 (1932); no. 2, p. 123.

[2] R. Muki and E. Sternberg, "Transfer of load from an edge-stiffener to a sheet – a reconsideration of Melan's problem," *Journal of Applied Mechanics*," vol. 34 (1967), no. 3, p. 679.

[3] R. Muki and E. Sternberg, "On the stress analysis of overlapping bonded elastic sheets," *International Journal of Solids and Structures*, vol. 4 (1968), no. 1, p. 75.

[4] R. Muki and E. Sternberg, "On the diffusion of load from a transverse tension-bar into a semi-infinite elastic sheet," *Journal of Applied Mechanics*, vol. 35 (1968), no. 4, p. 737.

[5] R. Muki and E. Sternberg, "On the diffusion of an axial load from an infinite cylindrical bar embedded in an elastic medium," *International Journal of Solids and Structures*, vol. 5 (1969), no. 6, p. 587.

[6] R. Muki and E. Sternberg, "Elastostatic load-transfer to a half-space from a partially embedded axially loaded rod," *International Journal of Solids and Structures*, vol. 6 (1970), no. 1, p. 69.

[7] E. Sternberg and R. Muki, "Load-absorption by a filament in a fiber-reinforced material," California Institute of Technology, October 1969. Technical Report No. 20, Contract Nonr-220(58), To appear in Zeitschrift für angewandte Mathematik und Physik.

[8] K. Girkmann, *Flachentragwerke*, Fifth Ed., Springer, Vienna, 1959.

[9] H. Bufler, "Zur Krafteinleitung in Scheiben über geschweisste oder geklebte Verbindungen," *Osterreichisches Ingenieur Archiv*, vol. 18 (1964), no. 3-4, p. 284.

[10] B. Budiansky and T. T. Wu, "Transfer of load to a sheet from a rivet-attached stiffener," *Journal of Mathematics and Physics*, vol. 40 (1961), no. 2, p. 142.

[11] F. J. Fisher, "Stress diffusion from axially loaded stiffeners into a cylindrical shells," *International Journal of Solids and Structures*, vol. 4 (1968), no. 12, p. 1181.

[12] W. T. Koiter, "On the diffusion of load from a stiffener into a sheet," *Quarterly Journal of Mechanics and Applied Mathematics*, vol. 8 (1955), no. 2, p. 164.

[13] E. Reissner, "Note on the problem of the distribution of stress in a thin stiffened elastic sheet," *Proceedings of the National Academy of Sciences*, vol. 26, (1940), p. 300.

[14] J. N. Goodier and C. S. Hsu, "Transmission of tension from a bar to a plate," *Journal of Applied Mechanics*, vol. 21 (1954), no. 2, p. 147.

[15] E. Melan, "Der Spannungszustand der durch eine Einzelkraft im Innern beanspruchten Halbscheibe," *Zeitschrift für angewandte Mathematik und Mechanik*, vol. 12 (1932), p. 343.

[16] N. I. Muskhelishvili, *Singular Integral Equations*, Second Ed., Noordhoff, Groningen, 1953.

[17] A. M. Hens, "De Inleiding van een Kracht op een Verstijver in een half-oneindige Plaat," Report of the Laboratorium voor Toegepaste Mechanica, Technische Hogeschool, Delft, 1957.

[18] E. Krahn, Discussion of Ref. [14], *Journal of Applied Mechanics*, vol. 22 (1955), no. 1, p. 139.

[19] E. J. LeFevre, D. R. J. Mudge, and J. F. Dickie, "An analysis of the distribution of tension in a bar attached to a plate," *Journal of Strain Analysis*, vol. 1 (1966), no. 5, p. 389.

[20] A. E. H. Love, *A treatise on the mathematical theory of elasticity*, Fourth Ed., Dover, New York, 1944.

[21] R. D. Mindlin, "Force at a point in the interior of a semi-infinite solid," *Physics*, vol. 7 (1936), p. 195.

[22] R. D. Mindlin, "Force at a point in the interior of a semi-infinite solid," *Proceedings, First Midwestern Conference of Solid Mechanics*, Urbana, Illinois, 1953, p. 56.

[23] L. J. Cohen and J. P. Romualdi, "Stress, strain and displacement fields in a composite material reinforced with discontinuous fibers," *Journal of the Franklin Institute*, vol. 284 (1967), no. 6, p. 388.

[24] R. Muki and E. Sternberg, "Note on an asymptotic property of solutions to a class of Fredholm integral equations," *Quarterly of Applied Mathematics*, vol. 28 (1970), no. 2, p. 277.